Article:
Kaiser, M, Chalapala, S, Gorzelanny, C et al. (2 more authors) (2016) The Effect of Capsaicin Derivatives on Tight-Junction Integrity and Permeability of Madin-Darby Canine Kidney Cells. Journal of Pharmaceutical Sciences, 105 (2). pp. 630-638. ISSN 0022-3549

https://doi.org/10.1016/j.xphs.2015.10.017

The effect of capsaicin derivatives on tight-junction integrity and permeability of MDCK cells

Kaiser M.[1], Chalapala S.[2], Gorzelanny C.[3], Perali R.S. [2*], Goycoolea F.M.[1*]

1: Institute of Plant Biology and Biotechnology (IBBP), Westfälische Wilhelms-Universität Münster, Schlossgarten 3, Münster 48149, Germany

2: School of Chemistry, University of Hyderabad, Hyderabad 500 046, India

3: Experimental Dermatology, Department of Dermatology, Medical Faculty Mannheim, Heidelberg University, Theodor-Kutzer-Ufer 1-3, Mannheim 68167, Germany

*= corresponding authors

Abstract

Capsaicin is known to interfere with tight junctions (TJ) of epithelial cells and therefore to enhance paracellular permeability of poorly absorbable drugs. However, due to its low water solubility, pungency and cytotoxicity its pharmacological use is limited. In this study, we investigated the effect of capsaicin derivatives of synthetic (*e.g.,* 10-hydroxy-N-(4-hydroxy-3-methoxybenzyl)decanamide, etc.) and natural (olvanil and dihydrocapsicin) origin on MDCK-C7 cells. Impedance spectroscopy was used to determine the transepithelial electrical resistance and the capacitance. Permeability assays with FITC-dextran were carried out to evaluate the impact on cell permeability. The results show that lipophilicity could play an important role for the interference with TJ and that the mechanism is independent from the ion channel TRPV 1 and hence, on the flux of calcium into the cells. In summary, we synthesized four derivatives of capsaicin of lower lipophilicity and compared their properties with other well-known vanilloids. We show that these compounds are able to enhance the permeability of a hydrophilic macromolecule, by opening the TJ for a shorter time than capsaicin. This behavior is dependent on the lipophilicity of the molecule. Understanding of these phenomena may lead to better control of administration of therapeutic molecules.

Keywords: MDCK cells, permeability, drug design, structure-activity relationship, solubility

Introduction

Capsaicin is known for its pungent taste and occurs in Nature as a constituent of chili peppers. It stimulates the TRPV-1 receptor, a relatively non-selective calcium channel, which is responsible for the sensation of heat [1]. Capsaicin is known to have versatile therapeutic effects like the treatment of chronic pain via the desensitization of afferent sensory neurons [2]. Other applications are the control of body temperature or as anti-obesity drug [3, 4]. More recently it has been discovered that capsaicin has a profound reversible opening effect on cellular tight junctions (TJ) [5]. This rigid cell connecting network of transmembrane proteins which is linked to the actin skeleton can be found in epithelial and endothelial tissues [6]. It serves as a protection mechanism to control the permeation of unknown compounds. Especially hydrophilic macromolecular drugs (e.g., proteins, polysaccharide, polynucleotides, etc.) are often unable to cross this barrier [7]. The property to reversibly open TJ makes capsaicin a potential permeability enhancer for drugs with a poor bioavailability [8-10]. However, the use of capsaicin also entails several drawbacks associated to its strong pungency and known cytotoxicity [11]. The application of high doses is not tolerable, especially in case of sensitive administration routes like the nasal or oral mucosae. Furthermore, its lipophilic character causes solubility difficulties when handling the compound in aqueous environments [12], which complicates a precise administration. Our previous studies in MDCK-C7 cells monolayers have shown that capsaicin is able to open reversible TJ for a time span of more than 10 h even at lower concentrations (≤ 500 mM) [10]. For a specific uptake of the delivered drug an immediate cell response and a very short time of opening would be advantageous to reduce the permeation of undesired substances. Based in this, we reasoned that it would be appropriate to modify the structure of capsaicin to improve its properties for the desired application. In the past, various capsaicin analogues have been synthesized mainly with the goal to find new agonists and antagonists [13-15]. Later, resiniferatoxin [16], an agonist which is 3 to 4 orders of magnitude more potent than capsaicin, and capsazepine [17], the first known antagonist, have been discovered. Also the structure-function relationship between different analogues and the TRPV1 activation has been studied [18-21]. It has been found that different analogues induce varying profiles of calcium release inside cells [22] and furthermore that too high hydrophilicity or hydrophobicity reduces the pungency of a compound [15, 23]. This can be explained by different permeability behaviors of compounds of different polarity through the cell membrane [23]. TRPV 1 receptors are also

expressed in the endoplasmatic reticulum and can release calcium ions from internal storages [18, 24]. In light of this, it has been hypothesized that different permeability behaviors influence also the release profile of intracellular calcium ions [25], which could in turn also affect other responses of the cell. Our goal was to establish a comparison between molecular features of capsaicin derivatives of synthetic and natural origin, and their biological activities in mammalian cells. In particular, we addressed the influence of these compounds on the paracellular transport of a model hydrophilic macromolecule (FITC-dextran). We aimed to shorten the duration of the TJ opening effect in comparison to capsaicin, thus facilitating a narrow time window of enhanced cell permeability. To this end, we synthesized four capsaicin analogues (**13, 14, 19, 20**) which have a low lipophilicity and also included capsaicin **21**, vanillin **1**, dihydrocapsaicin **22** nonivamide **23** and olvanil **24** in the study (Figure 1). We used the MDCK-C7 cell line as it is known to form a barrier of high integrity [26]. Impedance spectroscopy measurements, using a CellZscope device [27] for online measurements, were performed to determine the transepithelial electrical resistance (TEER) and the capacitance (C_{CL}). To investigate permeation of a model macromolecule (FITC-dextran 4000 Da), cell permeability assays using were carried out. Furthermore, the influx of calcium into the cells was investigated. Our study shows that different derivatives of capsaicin modify the effect of reversible TJ opening and molecular transport.

Experimental section

General Experimental Methods:

All the chemicals were purchased from Spectrochem, Avra, Merck and Sigma-Aldrich Chemical Companies and were of the highest purity. Capsaicin, dihydrocapsaicin, nonivamide and olvanil were purchased from Sigma-Aldrich (Steinheim, Germany). The protocol of synthesis of the compounds **13**, **14**, **19** and **20** is described in the Supporting Information.

Cell culture

MDCK-C7 cell line was cultured using MEM supplemented with 10% of fetal bovine serum, 1% of L-glutamine (200 mM) and 1% of penicillin-streptomycin (10000 units penicillin, 10000 units streptomycin in 0.9% NaCl) in 75 cm² flasks. The cultures were kept in an incubator set to 5% of CO2 and 37°C (Sanyo MCO-19AIC, Panasonic Biomedical Sales Europe BV., AZ Etten Leur, Netherlands). The passages 41 to

47 were used for all of the experiments. Those were carried out as independent triplicates on different days. After forming a confluent monolayer the cells were rinsed with 10 ml of PBS and trypsinized with 10 ml of trypsin buffer (0.05% trypsin EDTA). The trypsin buffer was diluted after detachment with 10 ml of cell culture medium. The cells were centrifuged at 1000 rpm for 5 min in a falcon tube (Rotina 420 R, Hettich GmbH, Tuttlingen, Germany). Supernatant was removed and the cell pellet was resuspended in 1 ml of cell culture medium. For counting 10 µl of cell suspension was diluted with 90 µl of trypan blue and transferred to an improved Neubauer chamber. Afterwards the cells were used for experiments. For subculture the cells were split in the ratio of 1:10.

Electrical impedance measurements

The CellZscope® (nanoAnalytics, Münster, Germany), an automated impedance spectrometer, was used to determine the TEER and the capacitance C_{CL} of a cell monolayer. Into the basolateral chamber of transwell Permeable Supports (12 mm Transwell with a 0.4 µm pore polycarbonate membrane insert; Corning Inc., New York, USA) approximately 1.5 ml of cell culture medium was filled. The apical compartment was loaded with 500 µl of cell suspension for seeding. A density of ≈25000 cells per well was chosen. The cells were allowed to form a monolayer for 4 days. One day prior to the experiment, every well was filled with 1.5 ml of supplement free medium. The cell culture medium of the supports was also replaced in the apical compartment by serum free medium. The membranes were transferred into the device and allowed to acclimate in the incubator and to reach a constant resistance of at least ≈5000 Ω*cm². By replacing 250 µl of the medium in the apical chamber by the sample dissolved in medium with the double of the desired concentration the experiment was started. The resistance and capacitance was continuously measured for 24 hours. The normalized TEER and capacitance was calculated according to the following equation (Eq. 1):

$$\text{Normalized TEER} = \frac{1}{3}\sum_{j=1}^{3}\left(\frac{\text{Sample}_j}{\left(\frac{1}{3}\sum_{i=1}^{3}\text{Control}_i\right)}\right) \quad (1)$$

Permeability assay

For the experiment cells were seeded on transwells with a density of 25000 cells/well. As transport medium modified MEM without phenol red supplemented with 1% L-glutamine, 1% of

penicillin/streptomycin and 10% FCS was used. As described previously for the TEER experiments the same volumes of medium were used to fill the compartments. The cells were cultured for 4 days to develop confluent monolayers. Afterwards the medium was exchanged with serum free transport cell growth medium and allowed to acclimate overnight. After acclimation TEER was determined for the transwells. Only filters with an electrical resistance of more than 5000 Ω*cm² were used for further experiments. To start the experiment half of the medium of the apical chamber was replaced by the same medium containing a twice as high sample concentration compared to the desired value and 37.5 µl of 50 mg/ml solution of fluorescein isothiocyanate-dextran (FITC-dextran, molecular weight 4000 Da, FITC:Glucose 1:250, Sigma-Aldrich GmbH, Steinheim, Germany). Aliquots of 100 µl of the medium in the basolateral chamber were collected after 1, 3, 5, 7, 9 and 24 hours and replaced with new medium. The aliquots were transferred into a 96-well plate (UV star black f-bottom, chimney well, µ clear, Greiner Bio-one GmbH, Frickenhausen, Germany) and fluorescence (λ_{ex} = 485 nm, λ_{em} = 520 nm) was measured in a in a microplate reader (Safire, Tecan AG, Salzburg, Austria). P_{app} was calculated using the following equation (Eq. 2):

$$P_{app} = V_r \times \frac{dC}{dt} \times \frac{1}{AC_0} \quad (2)$$

The experiment was carried out as four independent replicates with three technical replicates each.

Calcium influx measurements

Cells were seeded to form a confluent monolayer in an 8-well microscopy slide (µ-Slide 8 Well ibiTreat, ibidi GmbH, Munich, Germany) and allowed to attach to the surface overnight. After a washing step with supplement free medium each well was filled with 100 µl of medium containing Fluo-4 (1µl of 5 mM stock solution in 1 ml). The cells were incubated for 20 minutes. To remove the excess of dye the cells were rinsed with HEPES-buffered Ringer's solution (10 mM HEPES, 5 mM glucose, 1 mM $CaCl_2$, 1 mM $MgCl_2$, 5 mM KCl, 140 mM NaCl). Afterwards, 200 µl of HEPES buffer was filled in every well and the slide was immediately used for the experiment. Microscopy was performed using SIFM using an inverted fluorescence microscope (AxioObserver.Z1, Zeiss, Jena, Germany) equipped with a structured illumination module (ApoTome, Jena, Germany). A time lapse measurement was started (~0.88 frames/second). After recording about 20 frames 100 µl of sample containing 375 µM of test substance

was added using a pipette to reach an overall concentration of 125 µM. The time lapse was continued for around 5 minutes. For further analysis the images were processed with ImageJ. The images were normalized with a background subtraction using a rolling ball algorithm (ball radius = 500 pixels). Afterwards the brightness was adjusted. The overall brightness of the image was plotted over time and the brightness value before the addition was defined as zero.

Estimation of Log P values

Theoretical Log P values have been calculated using ChemBioDraw Ultra version 14.0.0.117 (Perkin Elmer Inc., Waltham, USA).

Data analysis

Statistical analysis of biological experiments was performed using Prism version 6.0c (GraphPad Software Inc., La Jolla, USA). All experiments have been statistically analyzed using non-parametric tests. For unpaired tests the Kruskal-Wallis test was applied and for paired tests the Friedman test was used. All biological experiments were conducted at least in triplicate.

Results

In this study we have investigated, in addition well-known capsaicin derivatives, the properties of four new derivatives with different hydrophilic groups in the aliphatic chain. Our reasoning for this was to gain a deeper understanding of the role of the length and molecular features of the aliphatic chain of vanilloids on their biological activity on epithelial cells. In particular we were interested in the paracellular permeability across monolayers of MDCK-C7 cells.

Estimation of theoretical Log P values

To estimate lipophilicity of the derivatives theoretical Log P values were calculated. The theoretical Log P values are shown in Figure 1. The lowest Log P values were found for the synthesized compounds **13** (Log P: 1.2) and **19** (Log P: 0.73). Then vanillin **1** had the next higher Log P value (Log P: 1.27). The other two synthesized compounds **14** (Log P: 2.87) and **20** (Log P: 2.4) followed. Nonivamide **23** (Log P: 3.65),

capsaicin **21** (Log P: 3.66) and dihydrocapsaicin **22** (Log P: 3.98) were the compounds with the next higher Log P values. Olvanil **24** (Log P: 7.09) had the highest value of all compounds.

Cytotoxicity studies

To find out the influence of the investigated compounds on cell viability we applied different concentrations on a monolayer of cells seeded on filter membranes. The cell viability was evaluated by continuous capacitance (C_{CL}) measurements over 24 hours (Figure 2) using the CellZscope® instrument. The plots show the normalized C_{CL} profiles over time for all the tested compounds at varying concentrations. Inspection of the plots shows that the synthesized compounds **13**, **14**, **19** and **20** when applied at doses of 250 and 500 μM had no pronounced effect on C_{CL}. However, compound **19** when applied at 750 μM increased slightly the response after 5 h. Vanillin **1** did not induce any observable change of C_{CL} even at the highest dose. Olvanil **24** at concentrations 250 and 500 μM did not had any effect. At a concentration of 750 μM though, it exerted a noticeable effect which started at about 9 h and persisted until the time of the analysis elapsed. This was reflected by the progressive increase of the standard deviation of the C_{CL} values and also by a slight increase in C_{CL} seen after 20 h. In turn, dihydrocapsaicin **22** had a very pronounced effect. At a concentration of 250 μM the response decreased slightly in the time course of the measurement until about 12 hours down to a value of 0.9. Beyond this time point it slightly recovered but did not reach its initial value. At a concentration of 500 μM, a strong sudden decrease can be appreciated in the beginning of the assay. After ~5 h the C_{CL} increased rapidly to a value of 5.0 with no further change beyond this point. At a concentration of 750 μM, a sudden increase occurred 1 h after the beginning of the measurement and reached a steady value of ~10.0. For nonivamide **23** there was a dose-dependent decrease of the C_{CL} traces. At a concentration of 250 μM this effect was comparable to the behavior after treatment with dihydrocapsaicin **22** at similar concentration. By contrast, at the higher concentrations the decrease in capacitance became more pronounced and also the endpoint C_{CL} values were lower than the initial ones. Also the behavior of capsaicin **21** at 500 μM was similar to nonivamide **23**.

Effect of compounds on TEER

The changes in TEER behavior were also studied concomitant to the C_{CL} measurements. In Figure 3 the normalized TEER is shown over a time span of 24 hours. The synthesized compounds (**13, 14, 19** and **20)**

showed a comparable effect on the normalized TEER behavior. Almost immediately after beginning of the measurement the TEER started to decrease and reached its minimum value after about two hours. The values reached were between 0.8 and 0.6 and compound **14** had the most prominent effect followed by compound **20**. The minima in TEER was followed by an increase to a value of ~0.90 which was reached after about 3 h for all the synthesized substances. Beyond this point the values continued increasing moderately over time. During this process the initial values were exceeded slightly. A dose dependency was not observable for any of these compounds. In case of vanillin **1** a similar behavior was visible with the difference that the decrease was far less prominent compared to the compounds **13**, **14**, **19** and **20**. The minimum TEER value for vanillin **1** was about ~0.95 and also in this case no dose dependency was observable. For olvanil **24** there was a minor increase of the TEER visible starting from 4 h. After 9 h at a concentration of 750 µM a monotonic decrease of the TEER occurred that continued until the end of the experiment. Dihydrocapsaicin **22** applied at a concentration of 250 µM, led to a sudden increase of the TEER at the beginning of the experiment, followed by a decrease that described 3 waves, with minima at ~1 (TEER: ~ 0.75), ~4 (TEER: ~ 0.6) and ~10 hours (TEER: ~ 0.5). Afterwards, the TEER increased and exceeded the initial value at about 1.5-fold. At higher concentrations dihydrocapsaicin **22** caused a total loss of the TEER. Nonivamide **23** at a concentration of 250 µM had a comparable effect to the one observed for dihydrocapsaicin **22**. At 500 µM the overall effect was more pronounced while at a concentration of 750 µM the TEER did not recover fully. Capsaicin **21** at a concentration of 500 µM showed a similar effect as that of nonivamide **23** at the same concentration.

Permeability studies

We conducted permeability assays across cell monolayers by applying the vanilloid compounds at a concentration of 500 µM. FITC-labeled dextran served as a probe to quantify permeability of a model macromolecule. Values of the amount of FITC-dextran were calculated after 9 and 24 h (Figure 4a) along with the relative permeability coefficient calculated at the time point of 9 h (Figure 4b). In both figures the compounds are aligned according with ascending Log P values. For the cumulative transport after 9 h (Figure 4a) it is worth noticing that all the investigated substances enhanced the amount of permeated probe with respect to the control. However, out of the synthesized compounds only **14** was to reach statistical significance ($P \leq 0.001$). Also capsaicin **21** ($P \leq 0.0001$), nonivamide **23** ($P \leq 0.0001$), and

olvanil **24** ($P \leq 0.01$) increased the permeability of FITC-dextran in a statistically significant manner. After 24 h a significant enhancement was not visible anymore for compound **14** while the other substances did maintain this behavior. Dihydrocapsaicin **22** enhanced the permeability very drastically at both of the time points investigated ($P \leq 0.0001$). Regarding the relative permeability coefficients estimated after 9 h (Figure 4b) notice that the compounds **13, 14, 19** and **20** enhanced the permeability in a range between 1.2 and 1.6 fold in comparison to the control. Especially compound **14** showed a statistically significant permeability increasing effect ($P \leq 0.01$). Also in case of vanillin **1** a slight but not statistically significant increase (1.2-fold) after 9 h was observable. Capsaicin **21** and nonivamide **23** showed a comparable behavior. Both compounds increased significantly (capsaicin **21**: $P \leq 0.01$, Nonivamide **23**: $P \leq 0.001$) the permeability by about 1.6-fold in comparison to the control. Olvanil **24** increased the permeability significantly after 9 h to around 1.9 ($P \leq 0.0001$). In case of dihydrocapsaicin **22** the permeability increased dramatically to a value of 350-fold ($P \leq 0.0001$). The inset in Figure 4b shows the dependency of the relative permeability on the Log P values of the investigated compounds. Notice that there is a strong linear correlation ($R^2 = 0.87$) between the permeability enhancement and the lipophilicity of the compounds.

In Figure 5 are plotted the time traces of relative cumulated permeated amount of probe along with the normalized TEER results for four representative compounds. A general consistent trend is appreciated between the increase in the amount of permeated probe and the decrease of TEER and vice versa. In case of nonivamide **23** the initial increase in TEER showed a reduced permeability at the beginning of the experiment. Also for compound **14** the relative permeability is reduced after 24 hours. The TEER crosses the initial value at around 6 hours. Increases in permeability were seen for nonivamide **23** especially between 5 and 10 h when the TEER reached its minimum value. Also for compound **14** a peak of permeability centered at ~3 h was accompanied by the drop in TEER after ~2 h. In case of vanillin **1** the permeability remained close to the initial value consistent with a minor change in TEER. By contrast with nonivamide **23** and compound **14**, olvanil **24** did enhance dramatically the permeability of the probe without any major effect on the TEER. Notice that the enhancement of permeability started at the same time as the minor TEER increase at around 4 hours.

Study of Calcium (Ca^{2+}) influx

The microscopy study in Figure 6 describes the calcium (Ca^{2+}) influx behavior of MDCK-C7 after the stimulation with the synthesized compounds **13**, **14**, **19**, and **20**, and capsaicin **21** (video file available as Supporting Information). To investigate this behavior the cells were loaded with a dye (Fluo-4) which starts to fluoresce after complexation with calcium. The figure shows the cell monolayer before and after the stimulation with the different substances. The images for the stimulated cells always show the maximal response observed. The upper panels correspond the micrographs for the control treatments, namely HEPES buffer (negative control), ionomycin (positive control), and capsaicin **21** (reference compound). For the negative control no change of fluorescence was noticed. As positive control we applied ionomycin, known to transport calcium across cellular membranes, and it showed a strong increase in fluorescence after the end of the assay (24 s). By contrast, capsaicin and the investigated substances did not show any increase in fluorescence after the stimulation of the cells when at a concentration of 125 µM. On the panel shown at the right side of the micrographs, the evolution of the fluorescence intensity during the course of the experiment is plotted. We also carried out a PCR assay to analyze the presence of the TRPV 1 receptor in the investigated cell line. There was no evidence of its expression under the conditions applied (see Supporting Information).

Discussion

In this study, we addressed the effect of various capsaicin derivatives from natural and synthetic origin on the drug permeability of MDCK-C7 cell monolayers. To this end, biophysical combined with biological methods have been used. We have chosen the MDCK-C7 cell line because it is a commonly used *in vitro* model of an epithelial barrier and for drug transport. Also it is suitable for impedance spectroscopy studies on cell monolayers [8, 10, 28]. It has been argued that the biological effects of capsaicin on epithelial cells are general, as previously shown for Caco-2 and MDCK cells [8].

We evaluated the cytotoxic response of the studied compounds from the capacitance values (C_{CL}) determined by impedance spectroscopy, as documented elswhere [29]. Also, the C_{CL} parameter is known to be a probe of cell adhesion processes on substrates and changes of cell shape [30]. In a previous study, we used this method along with a conventional metabolic competence assay (MTT), as reference, to assess

the cytotoxicity of capsaicin, and found that the results from both methods were comparable [10]. The study shows that the newly synthesized compounds **13**, **14**, **19** and **20** did not exhibit any cytotoxic properties at any of the tested concentrations. Also vanillin **1** showed a similar behavior. In case of olvanil **24** a change in the morphology of the cell monolayer was observable at a concentration of 750 µM with an onset time of 9 h. It is not clear in this case if the cells were harmed as the increase in capacitance is not pronounced enough. Furthermore, the TEER values also indicated that there was no complete disruption of the integrity of the cell monolayer which suggests that it was still intact. For nonivamide **23** and capsaicin **21** a slight dose-dependent decrease in capacitance was visible. The slight decrease of capacitance could be a result of an alteration of the physical and/or morphological properties [30]. This modification might be directly connected with the pronounced decrease in TEER induced by these compounds (Figure 2). These results are in general agreement with our own parallel studies using Caco-2 and TR146 epithelial cells [31, 32]. Also dihydrocapsaicin **22** showed a comparable decrease in capacitance at a sub lethal concentration of 250 µM, while higher concentrations lead to detachment of the dead cells as evidenced by the pronounced increase of capacitance.

The TEER results for capsaicin **21** are in close agreement with our previous studies where we investigated the profiles for a wider range of concentrations [10]. For all synthesized compounds an initial decrease of TJ integrity was observed, but not for nonivamide **23**, capsaicin **21** or dihydrocapsaicin **22**. Also a dose dependency of the observed effects was not visible for the synthesized compounds as it was for the other derivatives. Olvanil **24,** in contrast to all the other tested substances, initiated a decrease of TEER starting at ~ 9 h. This cannot be attributed to cytotoxicity as the capacitance remained unaffected. The long response time observed may be related to the high lipophilicity of olvanil **24** (i.e., Log P = 7.09). A longer retention in the cell membrane could explain the delayed onset of response, as previously suggested [23]. All the compounds showing a reversible decrease of TEER recovered to a higher value than the initial. This also suggests that the cell morphology could be affected as already indicated for the capacitance results.

Permeability studies support the findings of the TEER measurements. Notice that after 9 h there was an increase of P_{app} visible for all the studied compounds which induced a decrease of TEER. However, for compounds **13**, **19** and **20** this effect was not statistically significant, by contrast with compound **14** which

showed a significant P_{app} increase. Also, the cumulated transported amount of probe increased at time points where TEER was reduced (Figure 5). Olvanil **24** was an exception as P_{app} increased even without a major TEER decrease at comparable concentrations. After 24 hours all compounds which did not show a permanent TEER decreasing effect also did not increase permeability values. It can be hypothesized that a possible morphological change after initial decrease of the TEER even slowed down permeability as TEER exceeds the initial value. This would explain why the cumulated transported amount of the probe approaches again the control value for compound **14** (Figure 5). Olvanil **24** shows a very high permeability after 24 hours which cannot be explained within the present study as TEER values do not show a decrease. Nevertheless a cellular response at the time point of 9 hours was evident in case of capacitance and TEER. This time region also marks the change in permeability profile (Figure 4).

Enhancement of calcium uptake was observed neither for capsaicin nor for the newly synthesized compounds (Figure 6). This allows the conclusion that the mechanism of permeability enhancement is not dependent on the TRPV 1 receptor as it is furthermore not expressed in the investigated cell line (supporting information). In previous studies it has been shown that the activation of cofilin and the reduction of tight junction protein occludin is involved in the reversible effect of tight junction opening [8, 33].

The results suggest that lipophilicity could not only be important for the pungency of the capsaicionoids [15, 23] but also for the effect on paracellular permeability even though it can be assumed that the TRPV1 is not involved in the mechanism. We have gained evidence that the permeability coefficient increases with increasing Log P value for the non-cytotoxic compounds (Figure 4). As already stated in literature the presence of an optimum of lipophilicity for crossing the cell membrane [23] could play an important role for the effect on permeability. Experiments show that derivatives with a Log P value below 3 are not able to have a pronounced effect on TEER. A possible explanation could be that these compounds are not able to cross the cell membrane as effectively as compounds with a higher lipophilicity which reduces an interaction with intracellular structures. This could also explain the absence of a dose-dependent response for these compounds as only the area of the cell membrane could be involved which could be saturated already at the lowest amount investigated. Capsaicin **21**, nonivamide **23** and dihydrocapsaicin **22** show very pronounced effects on TEER and permeability as they are in the optimal range of lipophilicity. This has been shown for the pungency intensity of these compounds [23]. Olvanil **24**, a

compound with a very high Log P value, shows a very belated response. This could be explained by the long residence time of the compound inside the lipid bilayer of the membrane [23]. However, for this derivative an enhancement of permeability also at time points where TEER was not strongly affected was observed. Nevertheless it correlates with the general trend that a higher Log P value of the vanilloid increases the permeability of hydrophilic macromolecules. Recent studies have shown that the TRPV-4 receptor can influence TJ integrity via claudin-2 downregulation induced by hyperosmotic effects [34]. The calcium influx experiments did not show a positive result even though TRPV-4 was expressed in the investigated cell line. Whether vanilloid compounds addressed in this study have a different effect on the TRPV-4 channel remains to be investigated.

Conclusion

In summary, vanilloids which are less lipophilic than capsaicin **21** have been synthesized and compared with commercially available compounds aiming to improve some of the limitations of capsaicin and expand its pharmacological use. The new derivatives (**13**, **14**, **19** and **20**) are all able to open reversibly TJ for a short period of time upon administration which results in a short enhancement of permeability of FITC-dextran. This could allow a more precise enhancement of the absorption of a co-administered drug. Especially compound **14** seems to be a potential candidate for further studies as it increases the permeability significantly, shows no cytotoxicity and induces a very narrow profile of reversible tight junction opening. We venture to suggest that the observed biological activities of this compound stem on the molecular features, namely the length of the aliphatic chain along with the presence of a terminal hydroxyl group. We show for the first time that there is a consistent trend between the lipophilicity of vanilloid compounds and their effect on transport of a hydrophilic macromolecule. Less lipophilic compounds showed a rapid effect on TJ after administration and this is accompanied by a rapid increase of drug permeability. In addition, we show that the TRPV 1 receptor is not necessarily required to induce this effect in MDCK-C7 cells. The mechanism of this process has to be further evaluated and elucidated at the molecular level. We trust that the results of this study contribute to identify potential new non-toxic vanilloids which could be used as drug permeability enhancers.

Acknowledgements

We acknowledge support from DFG, Germany (Project GRK 1549 International Research Training Group 'Molecular and Cellular GlycoSciences') and from The Danish Agency for Science, Technology and Innovation, Denmark (FENAMI project 10-093456).

Literature Cited

1. Caterina MJ, Schumacher MA, Tominaga M, Rosen TA, Levine JD, Julius D 1997. The capsaicin receptor: A heat-activated ion channel in the pain pathway. Nature 389:816-824.

2. Jancsó N, Jancsó-Gábor A, Szolcsányi J 1967. Direct evidence for neurogenic inflammation and its prevention by denervation and by pretreatment with capsaicin. Br J Pharmacol 31:138-151.

3. Meghvansi MK, Siddiqui S, Khan MH, Gupta VK, Vairale MG, Gogoi HK, Singh L 2010. Naga chilli: A potential source of capsaicinoids with broad-spectrum ethnopharmacological applications. J Ethnopharmacol 132:1-14.

4. Zhang LL, Liu DY, Ma LQ, Luo ZD, Cao TB, Zhong J, Yan ZC, Wang LJ, Zhao ZG, Zhu SJ, Schrader M, Thilo F, Zhu ZM, Tepel M 2007. Activation of transient receptor potential vanilloid type-1 channel prevents adipogenesis and obesity. Circ Res 100:1063-1070.

5. Hu D, Easton A, Fraser P 2005. TRPV1 activation results in disruption of the blood-brain barrier in the rat. Br J Pharmacol 146:576-584.

6. Tsukita S, Furuse M, Itoh M 2001. Multifunctional strands in tight junctions. Nat Rev Mol Cell Bio 2:285-293.

7. Sonaje K, Lin K, Wang J, Mi F, Chen C, Juang J, Sung H 2010. Self-Assembled pH-Sensitive Nanoparticles: A Platform for Oral Delivery of Protein Drugs. Adv Funct Mater 20:3695-3700.

8. Shiobara T, Usui T, Han J, Isoda H, Nagumo Y 2013. The reversible increase in tight junction permeability induced by capsaicin is mediated via cofilin-actin cytoskeletal dynamics and decreased level of occludin. PLoS ONE 8(11):e79954.

9. Kaiser M, Goycoolea FM. 2014. Vanilloids and Their Effect on Mammalian Biological Barriers. In Gilliam B, editor. Capsaicin: Food Sources, Medical Uses and Health Implications: Nova Science Publishers. p 53-74.

10. Kaiser M, Pereira S, Pohl L, Ketelhut S, Kemper B, Gorzelanny C, Galla H-, Moerschbacher BM, Goycoolea FM 2015. Chitosan encapsulation modulates the effect of capsaicin on the tight junctions of MDCK cells. Sci Rep 5:10048.

11. Tsukura Y, Mori M, Hirotani Y, Ikeda K, Amano F, Kato R, Ijiri Y, Tanaka K 2007. Effects of capsaicin on cellular damage and monolayer permeability in human intestinal Caco-2 cells. Biol Pharm Bull 30:1982-1986.

12. Turgut C, Newby B-, Cutright TJ 2004. Determination of Optimal Water Solubility of Capsaicin for its Usage as a Non-toxic Antifoulant. Environ Sci Pollut R 11:7-10.

13. Walpole CSJ, Wrigglesworth R, Bevan S, Campbell EA, Dray A, James IF, Perkins MN, Reid DJ, Winter J 1993. Analogues of capsaicin with agonist activity as novel analgesic agents; structure-activity studies. 1. The aromatic "A-region". J Med Chem 36:2362-2372.

14. Walpole CSJ, Wrigglesworth R, Bevan S, Campbell EA, Dray A, James IF, Masdin KJ, Perkins MN, Winter J 1993. Analogues of capsaicin with agonist activity as novel analgesic agents; structure-activity studies. 2. The amide bond "B-region". J Med Chem 36:2373-2380.

15. Walpole CSJ, Wrigglesworth R, Bevan S, Campbell EA, Dray A, James LF, Masdin KJ, Perkins MN, Winter J 1993. Analogues of capsaicin with agonist activity as novel analgesic agents; structure-activity studies. 3. The hydrophobic side-chain "C-region". J Med Chem 36:2381-2389.

16. Szallasi A, Blumberg PM 1989. Resiniferatoxin, a phorbol-related diterpene, acts as an ultrapotent analog of capsaicin, the irritant constituent in red pepper. Neuroscience 30:515-520.

17. Bevan S, Hothi S, Hughes G, James IF, Rang HP, Shah K, Walpole CSJ, Yeats JC 1992. Capsazepine: A competitive antagonist of the sensory neurone excitant capsaicin. Br J Pharmacol 107:544-552.

18. Thomas KC, Ethirajan M, Shahrokh K, Sun H, Lee J, Cheatham III TE, Yost GS, Reilly CA 2011. Structure-activity relationship of capsaicin analogs and transient receptor potential vanilloid 1-mediated human lung epithelial cell toxicity. J Pharmacol Exp Ther 337:400-410.

19. Steinberg X, Lespay-Rebolledo C, Brauchi S 2014. A structural view of ligand-dependent activation in thermoTRP channels. Front Physiol 5:171.

20. Rusterholz DB 2006. Capsaicin, from hot to not; can new pain-relieving drugs be derived from this substance known to cause pain? J Chem Educ 83:1809-1815.

21. Huang X-, Xue J-, Jiang A-, Zhu H- 2013. Capsaicin and its analogues: Structure-activity relationship study. Curr Med Chem 20:2661-2672.

22. Tóth A, Wang Y, Kedei N, Tran R, Pearce LV, Kang S-, Jin M-, Choi H-, Lee J, Blumberg PM 2005. Different vanilloid agonists cause different patterns of calcium response in CHO cells heterologously expressing rat TRPV1. Life Sci 76:2921-2932.

23. Ursu D, Knopp K, Beattie RE, Liu B, Sher E 2010. Pungency of TRPV1 agonists is directly correlated with kinetics of receptor activation and lipophilicity. Eur J Pharmacol 641:114-122.

24. Cortright DW, Szallasi A 2004. Biochemical pharmacology of the vanilloid receptor TRPV1: An update. Eur J Biochem 271:1814-1819.

25. Blumberg PM, Pearce LV, Lee J 2011. TRPV1 activation is not an all-or-none event: TRPV1 partial agonism/antagonism and its regulatory modulation. Curr Top Med Chem 11:2151-2158.

26. Gekle M, Wünsch S, Oberleithner H, Silbernagl S 1994. Characterization of two MDCK-cell subtypes as a model system to study principal cell and intercalated cell properties. Pflugers Arch - Eur J Physiol 428:157-162.

27. Benson K, Cramer S, Galla H- 2013. Impedance-based cell monitoring: Barrier properties and beyond. Fluids Barriers CNS 10:5.

28. Irvine JD, Takahashi L, Lockhart K, Cheong J, Tolan JW, Selick HE, Grove JR 1999. MDCK (Madin-Darby canine kidney) cells: A tool for membrane permeability screening. J Pharm Sci 88:28-33.

29. Lee R, Kim J, Kim SY, Jang SM, Lee S-, Choi I-, Park SW, Shin J-, Yoo K- 2012. Capacitance-based assay for real-time monitoring of endocytosis and cell viability. Lab Chip 12:2377-2384.

30. Wegener J, Keese CR, Giaever I 2000. Electric cell-substrate impedance sensing (ECIS) as a noninvasive means to monitor the kinetics of cell spreading to artificial surfaces. Exp Cell Res 259:158-166.

31. Kaiser M, Kirsch B, Hauser H, Schneider D, Seuß-Baum I, Goycoolea FM 2015. In Vitro and Sensory Evaluation of Capsaicin-Loaded Nanoformulations. Plos One (in press) DOI:10.1371/journal.pone.0141017.

32. Kaiser M, Lankamp F, Goycoolea FM Nanoencapsulation of capsaicin attenuates the cytotoxic effect on Caco-2 cells. (unpublished data).

33. Nagumo Y, Han J, Arimoto M, Isoda H, Tanaka T 2007. Capsaicin induces cofilin dephosphorylation in human intestinal cells: The triggering role of cofilin in tight-junction signaling. Biochem Biophys Res Commun 355:520-525.

34. Ikari A, Fujii N, Hahakabe S, Hayashi H, Yamaguchi M, Yamazaki Y, Endo S, Matsunaga T, Sugatani J 2015. Hyperosmolarity-Induced Down-Regulation of Claudin-2 Mediated by Decrease in PKCβ-Dependent GATA-2 in MDCK Cells. J Cell Physiol 230:2776-2787.

Figure legends

Figure 1. Vanilloids which have been used for this study. The thereoretical Log P values were estimated.

Figure 2. Impedance spectroscopy measurements for determination of capacitance: Normalized capacitance in relation to the control for increasing concentrations over time. Color code: 250 µM: black; 500 µM: green; 750 µM: red. The plot shows mean values ± s.d. (n=3).

Figure 3. Impedance spectroscopy measurements for determination of TEER: Normalized TEER in relation to the control for increasing concentrations over time. Color code: 250 µM: black; 500 µM: green; 750 µM: red. The plot shows mean values ± s.d. (n=3).

Figure 4. Permeability assay with MDCK-C7 cells using FITC-dextran (MW= 4000 Da). Derivatives were investigated with a concentration of 500 µM. Cumulated permeated amounts of probe after 9 and 24 h (a), relative permeability coefficient in relation to the control (P_{app}) derived from the slopes of the transport curves after 9 hours (b). Compounds are aligned in increasing Log P. Inset shows the dependency of Log P and P_{app} of the investigated compounds. Mean values ± s.d., Statistical test: Kruskal-Wallis test (n=4, ** $p < 0.01$, *** $p < 0.001$, **** $p < 0.0001$).

Figure 5. Cumulative amount of dextran permeated plotted together with TEER behavior over time for representative derivatives at a concentration of 500 µM. Mean values ± s.d.. (TEER: n=3, Permeability: n=4).

Figure 6. Calcium (Ca^{2+}) influx measurements using Fluo-4 to quantify the amount of calcium fluxed into the cells. Image shows representative measurements. The samples were investigated at a concentration of 125 µM. Stimulated images show the maximum response of the cells. The fluorescence over time course of the experiment is plotted (Scale bar = 200 µM).

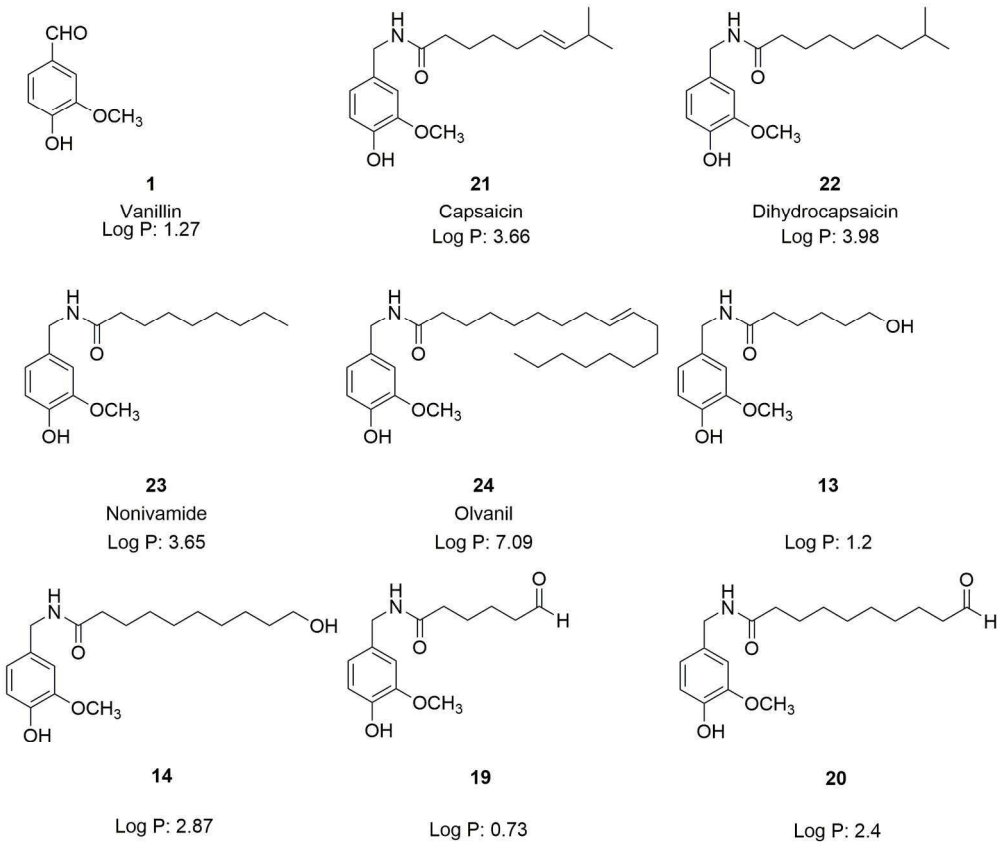

183x154mm (300 x 300 DPI)

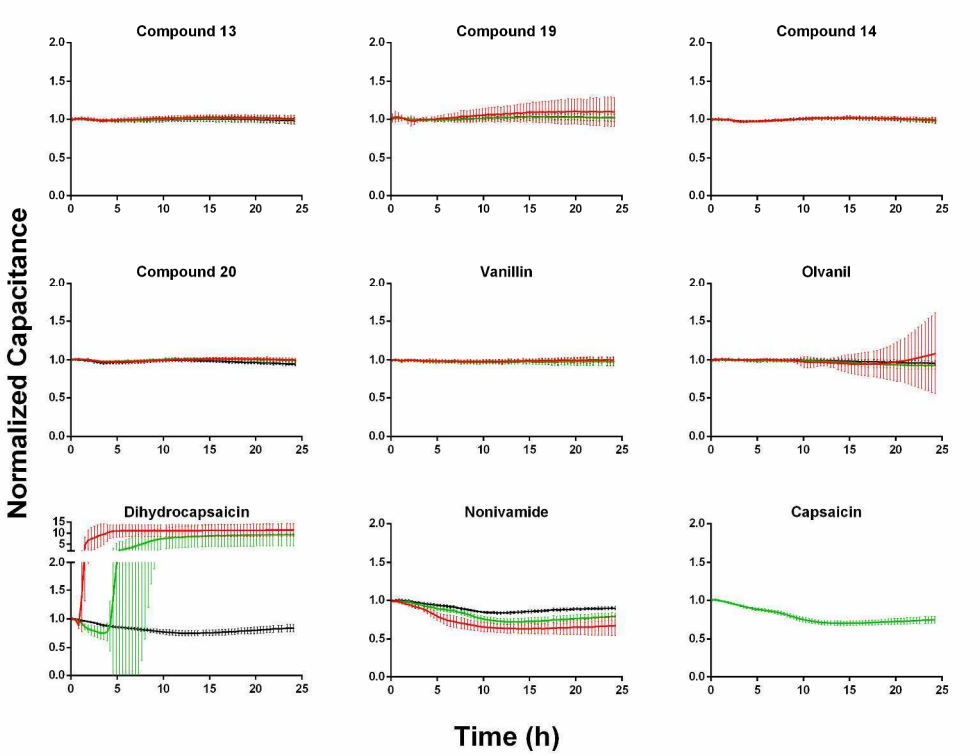

267x205mm (300 x 300 DPI)

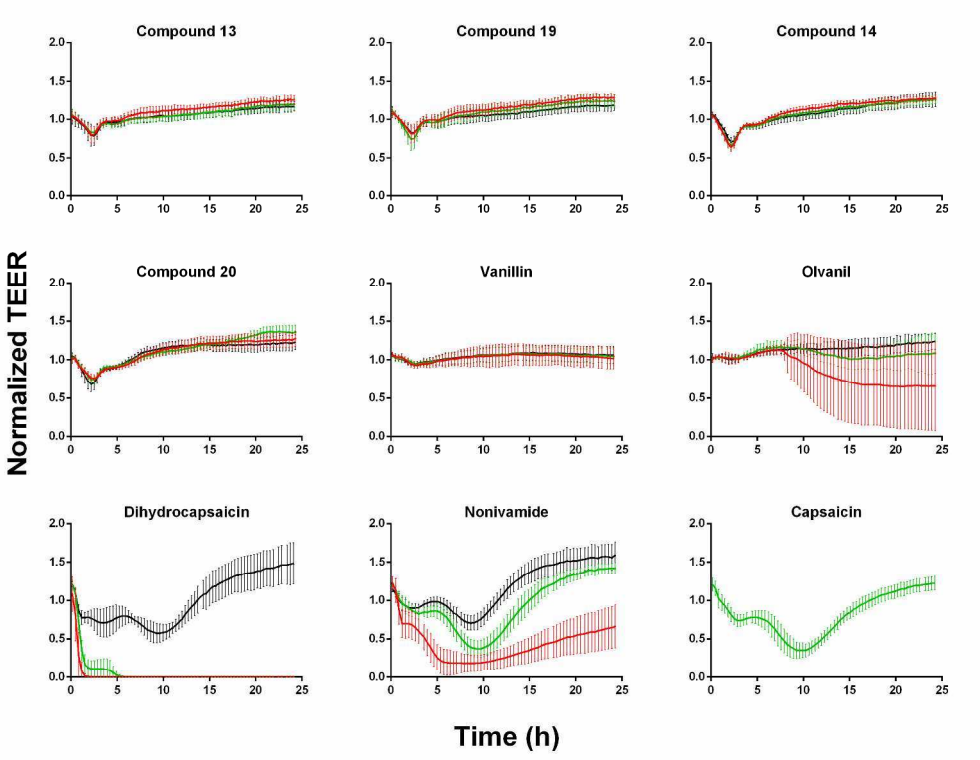

267x205mm (300 x 300 DPI)

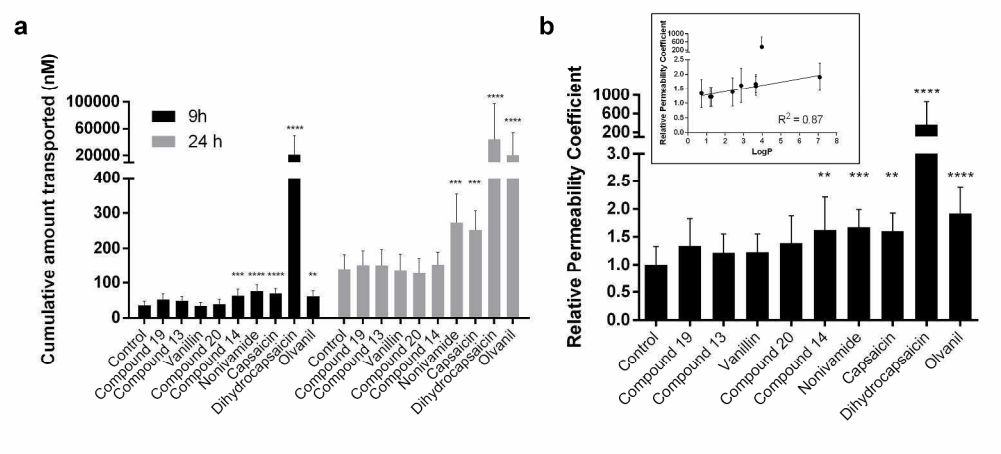

282x128mm (300 x 300 DPI)

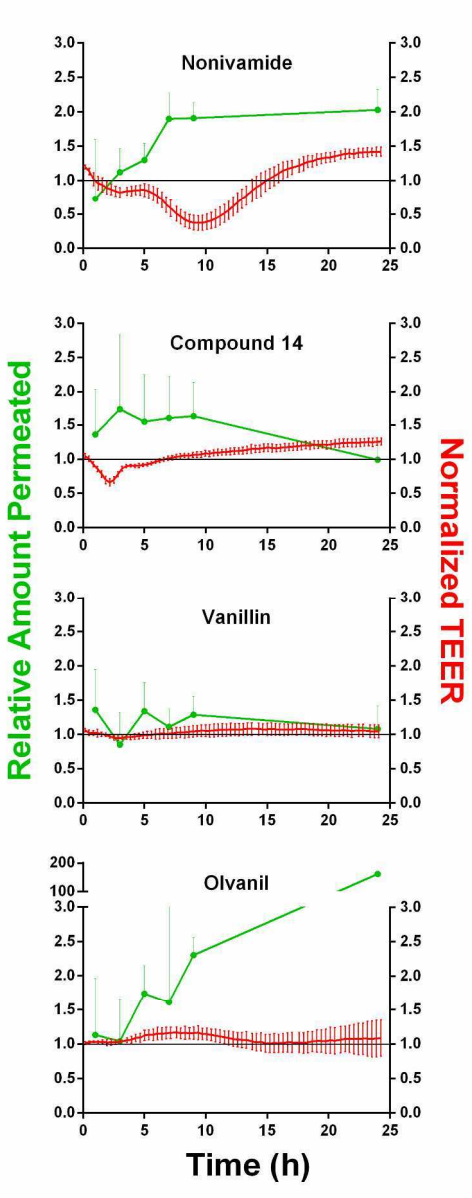

112x270mm (300 x 300 DPI)

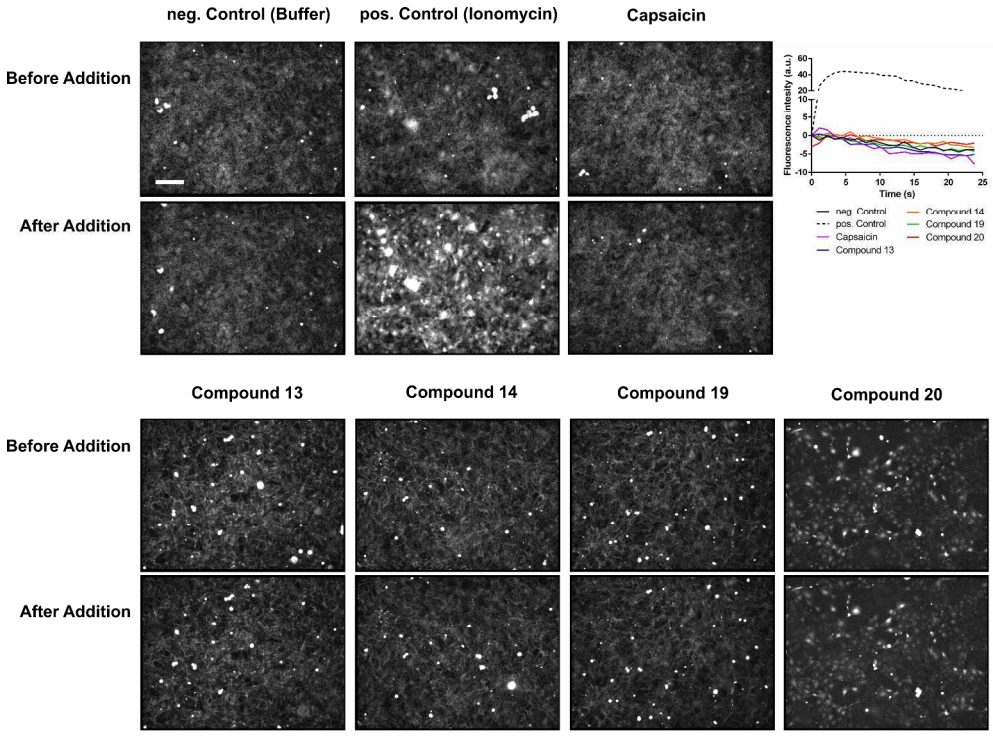

337x243mm (300 x 300 DPI)

The effect of capsaicin derivatives on tight-junction integrity of MDCK cells

Kaiser M.[1], Chalapala S.[2], Gorzelanny C.[3], Perali R.S.[2], Goycoolea F.M.[1*]

1: Institute of Plant Biology and Biotechnology (IBBP), Westfälische Wilhelms-Universität Münster, Schlossgarten 3, Münster 48149, Germany

2: School of Chemistry, University of Hyderabad, Hyderabad 500 046, India

3: Experimental Dermatology, Department of Dermatology, Medical Faculty Mannheim, Heidelberg University, Theodor-Kutzer-Ufer 1-3, Mannheim 68167, Germany

Supporting information

Contents:

Synthesis of capsaicin derivatives

The synthesis of the capsaicin derivatives was commenced starting from vanillin **1**. Thus, selective protection of the phenolic hydroxyl with a *tert*-butyldimethylsilyl (TBS) group resulted in aldehyde **2** which upon reaction with hydroxylamine hydrochloride provided the corresponding oxime **3** [1] in 85% yield. Pd/C mediated hydrogenation of **3** under hydrogen atmosphere gave the key intermediate amine **4** (Scheme 1).

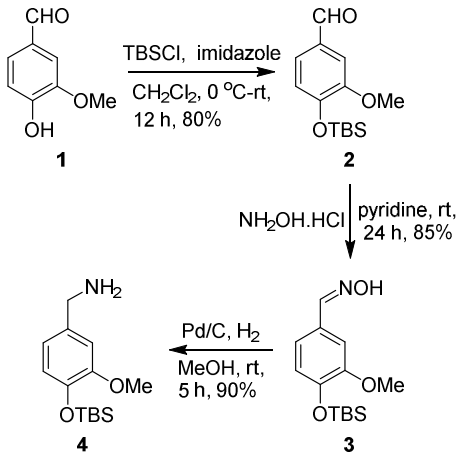

Scheme 1. Synthesis of vanillin derived amine **4**.

The aliphatic side chain precursors for the coupling reaction were synthesized from hexan 1,6-diol **5** and decan 1,10-diol **6**. Selective mono protection of the hydroxyl in **5** and **6** with TBSCl provided the alcohols **7** and **8** in good yield. Oxidation of the primary alcohol in **7** and **8** with pyridiniumdichromate (PDC) lead to the formation of carboxylic acids **9** and **10** (Scheme 2).

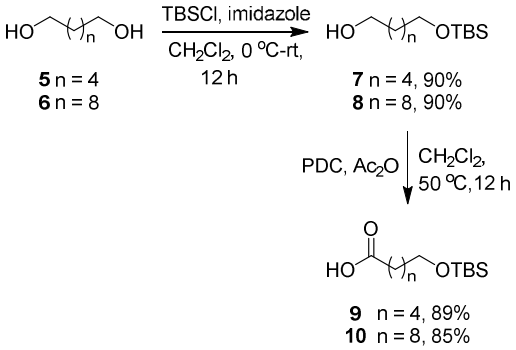

Scheme 2. Synthesis of carboxylic acids **9** and **10**.

EDCI (1-(3-dimethylaminopropyl-3-ethylcarbodiimide hydrochloride) mediated coupling reaction of **4** with carboxylic acids **9** and **10** furnished the corresponding amide derivatives **11** and **12**. Deprotection of both the TBS groups in **11** and **12** with TBAF in THF gave the capsaicin derivatives **13** and **14** in good yield (Scheme 3).

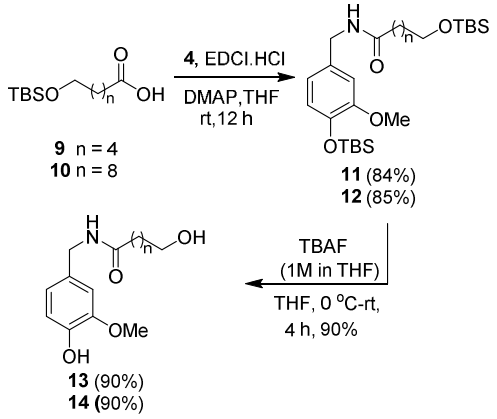

Scheme 3. Synthesis of capsaicin derivatives **13** and **14**.

On the other hand, selective deprotection of aliphatic OTBS group in **11** and **12** with $CeCl_3.7H_2O$ in refluxing acetonitrile provided the corresponding primary alcohols **15** and **16** [2]. Oxidation of the alcohol with pyridiniumdichromate provided the aldehydes **17** and **18**. Deprotection of phenolic TBS group in **17** and **18** with TBAF gave the corresponding capsaicin derivatives **19** and **20** (Scheme 4).

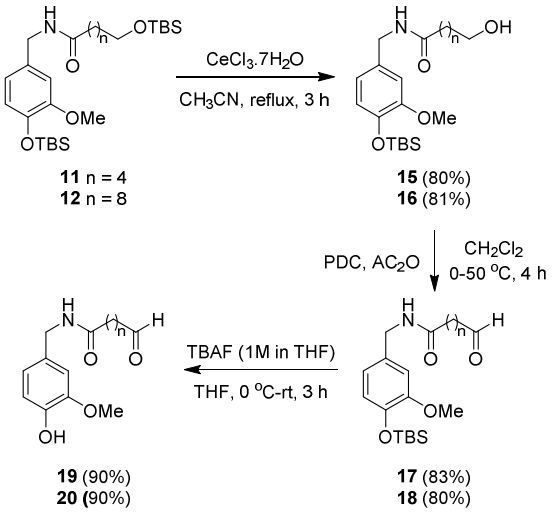

Scheme 4. Synthesis of capsaicin derivatives **19** and **20**.

Experimental Section Synthesis

The reactions were carried out under an inert atmosphere and monitored by thin-layer chromatography (TLC) using silica gel GF_{254} plates with detection by phosphomolybdic acid (PMA) stain and by ultra violet (UV) detection unless otherwise mentioned. Ethanol, THF, pyridine, methanol, acetonitrile and CH_2Cl_2 used in the reactions were distilled from dehydrating agents prior to use. Silica gel (100-200) was used for column chromatography. ^1H, ^{13}C spectra were recorded with Bruker 400 MHz or 500 MHz spectrometers in $CDCl_3$. ^1H NMR chemical shifts are reported in ppm (δ) with TMS as internal standard (δ = 0.00 ppm); ^{13}C NMR data are reported in chemical shifts with solvent reference ($CDCl_3$, δ = 77.00 ppm). IR spectra were recorded with a JASCO FT/IR-5300 spectrometer. High-resolution mass spectra were recorded with a Bruker maXis ESI-TOF spectrometer.

4-((*tert*-butyldimethylsilyl)oxy)-3-methoxybenzaldehyde (2):

To a stirred solution of compound **1** (5 g, 32.89 mmol) in dry dichloromethane (50 mL) was added imidazole (3.13 g, 46.05 mmol) and TBDMSCl (5.42 g, 36.17 mmol) at 0 ^oC, slowly warmed to room temperature, stirring was continued for 12 h at room temperature. After completion of the reaction, quenched with saturated ammonium chloride solution, mixture was diluted with CH_2Cl_2 (3x100m L), the organic layer was separated, finally washed with brine and dried over anhydrous sodium sulphate, filter, evaporation under reduced pressure provides the crude, which was purified by silica-gel column chromatography using hexane/ethyl acetate as eluents gave the compound **2** in 80% (7 g) yield. R_f = 0.66 in 20% EtOAc/Hexane.

^1H NMR (400 MHz, $CDCl_3$): δ 9.79 (s, 1H), 7.30-7.36 (m, 2H), 6.92 (d, *J* = 2.0 Hz, 1H), 3.82 (s, 3H), 0.95 (s, 9H), 0.14 (s, 6H) ppm. **^{13}C NMR (100 MHz, $CDCl_3$)**: δ 190.8, 151.5, 151.2, 130.9, 126.1, 120.6, 110.0, 55.3, 25.5, 18.4, -4.6 ppm.

4-((*tert*-butyldimethylsilyl)oxy)-3-methoxybenzaldehyde oxime (3):

To a stirred solution of compound **2** (6 g, 0.02 mmol) in dry pyridine (60 mL) was added hydroxyl amine hydrochloride (1.88 g, 0.028 mmol) at rt and stirring was continued for 12 h, after completion of the reaction pyridine was removed under reduced pressure, the obtained crude product was dissolved in chloroform 60 mL, washed with water, the aqueous layer was washed with chloroform (2x60 mL), the combined organic layer was washed with brine, dried over anhydrous sodium sulphate, filter and evaporation using rotary evaporator provided the crude product which was purified by using silica-gel column chromatography over hexane/ethyl acetate gave the compound **3** in 85% yield (5.5 g). R_f = 0.55 in 30% EtOAc/Hexane.

^{1}H NMR (400 MHz, $CDCl_3$): δ 9.68 (bs, 1H), 8.13 (s, 1H), 7.23 (d, *J* = 2.0 Hz, 1H), 6.97 (dd, *J* = 1.6 Hz, *J* = 8.0 Hz, 1H), 6.85 (d, *J* = 8.0 Hz, 1H), 3.83 (s, 3H), 1.02 (s, 9H), 0.19 (s, 6H) ppm. **^{13}C NMR (100 MHz, $CDCl_3$)**: δ 151.3, 150.4, 147.1, 125.6, 121.6, 120.8, 109.1, 55.4, 25.7, 18.5, -4.5 ppm.

(4-((*tert*-butyldimethylsilyl)oxy)-3-methoxyphenyl)methanamine (4):

To a stirred solution of compound **3** (5.5 g, 19.57 mmol) in methanol was added Pd/C (400 mg) then stirring was continued in presence H_2 atmosphere for 5 h at rt. After completion of the reaction Pd/C was filtered off using celite 545 using methanol, the filtrate was evaporated under reduced pressure followed by column chromatography over methanol/chloroform gave the compound **4** in 90% yield (4.7 g). R_f = 0.34 in 20% MeOH/$CHCl_3$.

^{1}H NMR (400 MHz, $CDCl_3$): δ 6.88 (s, 1H), 6.81 (d, *J* = 8.0 Hz, 1H), 6.76 (d, *J* = 8.0 Hz, 1H), 3.80 (s, 3H), 3.72 (s, 2H), 0.99 (s, 9H), 0.15 (s, 6H) ppm. **^{13}C NMR (100 MHz, $CDCl_3$)**: δ 150.9, 143.8, 136.5, 120.8, 119.2, 111.1, 55.4, 46.0, 25.7, 18.4, -4.6 ppm.

6-((*tert*-butyldimethylsilyl)oxy)hexan-1-ol (7):

Compound **7** was synthesized using the procedure described for compound **2** by taking **5** (2 g, 16.94 mmol) in 90% yield (3.5 g). R_f = 0.36 in 10% EtOAC/Hexane.

^{1}H NMR (400 MHz, $CDCl_3$): δ 3.56 (q, *J* = 6.8 Hz, *J* = 15.2 Hz, 4H), 1.76 (bs, 1H), 1.50-1.58 (m, 4H), 1.33 (t, *J* = 3.2 Hz, 4H) ppm. **^{13}C NMR (100 MHz, $CDCl_3$)**: δ 63.1, 62.8, 32.7, 32.7, 25.9, 25.6, 25.5, 18.3, -5.2 ppm.

10-((*tert*-butyldimethylsilyl)oxy)decan-1-ol (8):

Compound **8** was synthesized using the procedure described for compound **2** by taking **6** (5 g, 28.73 mmol) in 90% yield (7.4 g). R_f = 0.47 in 10% EtOAC/Hexane.

^{1}H NMR (500 MHz, $CDCl_3$): δ 3.56-3.61(m, 4H), 1.48-153(m, 4H), 1.26 (s, 12H), 0.87 (s, 9H), 0.02 (s, 6H) ppm. **^{13}C NMR (125 MHz, $CDCl_3$)**: δ 63.3, 62.9, 62.9, 32.8, 32.7, 29.5, 29.4, 25.9, 25.7, 25.7, 18.3 ppm.

6-((*tert*-butyldimethylsilyl)oxy)hexanoic acid (9):

To a stirred solution of compound **7** (3 g, 12.93 mmol) in dry DCM (40 mL) pyridinium dichromate (3.5 g, 9.56 mmol) at rt, followed by addition of acetic anhydride (43.96 mmol, 4.39 mL) at 0 ^oC, further stirring was continued at 50 ^oC for 5 h provided the compound **9** in 89% yield (2.85 g). R_f = 0.4 in 20% EtOAc/Hexane.

^{1}H NMR (400 MHz, $CDCl_3$): δ 9.27 (bs, 1H), 3.59 (t, *J* = 12.8 Hz, 2H), 2.32 (t, *J* = 7.2 Hz, 2H), 2.07 (s, 2H), 1.60-1.67 (m, 2H), 1.48-1.55 (m, 2H), 1.31-1.40 (m, 2H), 0.87 (s, 9H), 0.03 (s, 6H) ppm.

10-((*tert*-butyldimethylsilyl)oxy)decanoic acid (10):

To a stirred solution of compound **8** (5 g, 19.23 mmol) in dry CH_2Cl_2 (60 mL) pyridinium dichromate (5.3 g,14.23 mmol) at rt, followed by addition of acetic anhydride (65.38 mmol, 6.5 mL) at 0 ^oC, further stirring was continued at 50 ^oC for 5 h provided the compound **10** in 85% yield (4.9 g). R_f = 0.34 in 30% EtOAc/Hexane.

IR (NEAT): ν_{max} 2926, 2854, 1819, 1709, 1457, 1260, 1095 Cm^{-1}. **^{1}H NMR (400 MHz, $CDCl_3$)**: δ 3.57-3.61 (m, 2H), 2.42-2.46 (m, 2H), 1.64 (t, *J* = 6.8 Hz, 2H), 1.49 (d, *J* = 12.8 Hz, 2H), 1.29 (s, 12H), 0.89 (s, 9H), 0.04 (s, 6H) ppm. **^{13}C NMR (100 MHz, $CDCl_3$)**: δ 169.6, 63.3, 35.2, 32.8, 29.7, 29.3, 29.1, 28.8, 25.9, 25.7, 24.2, 18.3, -5.2 ppm. **HRMS (ESI)** calcd for $C_{16}H_{34}O_3Si$+Na 325.2175, found 325.2180.

6-((*tert*-butyldimethylsilyl)oxy)-*N*-(4-((*tert*-butyldimethylsilyl)oxy)-3-methoxybenzyl)hexanamide (11):

To a stirred solution of compounds **4** (500 mg, 1.87 mmol) and **9** (506 mg, 2.05 mmol) in dry THF (8 mL) was added EDCI.HCl (442 mg, 2.24 mmol) and DMAP (251 mg, 2.05 mmol) at 0 ^{o}C, slowly it warmed to room temperature, stirring was continued for 12 h at room temperature until the completion of the reaction, after completion of the reaction, reaction mixture was diluted with ethyl acetate, the organic layer was washed with water, brine, dried over sodium sulphate, filter and evaporated under reduced pressure gave crude compound which was further purified by using silica-gel column chromatography provided compound **11** in 83% yield (780 mg). R_f = 0.4 in 30% EtOAc/Hexane.

^{1}H NMR (400 MHz, $CDCl_3$): δ 6.75 (t, *J* = 8.4 Hz, 2H), 6.68 (d, *J* = 8.0 Hz, 1H), 6.03 (s, 1H), 4.32 (d, *J* = 5.6 Hz, 2H), 3.76 (s, 3H), 3.62 (t, *J* = 5.6 Hz, 2H), 2.28 (t, *J* = 7.2 Hz, 2H), 1.83 (t, *J* = 6.8 Hz, 2H), 1.24 (s, 2H), 0.97 (s, 9H), 0.85 (s, 9H), 0.12 (s, 6H), 0.00 (s, 6H) ppm. **^{13}C NMR (100 MHz, $CDCl_3$)**: δ 172.7, 151.0, 144.4, 131.8, 120.8, 120.1, 111.9, 62.2, 55.4, 43.4, 33.2, 29.7, 28.5, 25.9, 25.7, 18.4, 18.2, -4.6, -5.3 ppm.

10-((*tert*-butyldimethylsilyl)oxy)-N-(4-((*tert*-butyldimethylsilyl)oxy)-3-methoxybenzyl)decanamide (12):

To a stirred solution of compounds **4** (500 mg, 1.87 mmol) and **10** (622 mg, 2.05 mmol) in dry THF (8 mL) was added EDCI.HCl (442 mg, 2.24 mmol) and DMAP (251 mg, 2.05 mmol) at 0 ^{o}C, slowly it warmed to room temperature, stirring was continued for 12 h at room temperature until the completion of the reaction, after completion of the reaction reaction mixture was diluted with ethyl acetate, the organic layer was washed with water, brine, dried over sodium sulphate, filter and evaporated under reduced pressure gave crude compound which was further purified by using silica-gel column chromatography provided compound **12** in 85% yield (770 mg). R_f = 0.52 in 30% EtOAc/Hexane.

^{1}H NMR (400 MHz, $CDCl_3$): δ 6.75-6.79 (m, 2H), 6.68 (t, *J* = 1.6 Hz, 1H), 5.72 (s, 1H), 4.33 (d, *J* = 5.6 Hz, 2H), 3.77 (s, 3H), 3.56-3.59 (m, 2H), 2.17 (dd, *J* = 7.6 Hz, J = 12.4 Hz, 2H), 1.64 (bs, 2H), 1.49 (bs, 2H), 1.25 (d, *J* = 8.8 Hz, 10H), 0.98 (s, 9H), 0.88 (s, 9H), 013 (s, 6H), 0.03 (s, 6H) ppm. **^{13}C NMR (100 MHz,**

$CDCl_3$): δ 172.9, 151.0, 144.4, 131.8, 120.8, 120.1, 111.8, 63.3, 55.4, 43.4, 36.8, 32.8, 29.7, 29.4, 29.3, 29.3, 25.9, 25.8, 25.7, 18.4, 18.3, -4.6, -5.2 ppm.

6-hydroxy-*N*-(4-hydroxy-3-methoxybenzyl)hexanamide (13):

To a stirred solution of compound **11** (400 mg, 0.5472 mmol), in dry THF (10 mL) was added TBAF 1M in THF (0.87 mmol, 0.9 mL) at 0 ^{o}C, then stirring was continued for 4h at rt, after 4h quenched with saturated ammonium chloride solution, extracted with ethyl acetate, finally with brine, dried and evaporated provided the crude product which was purified by column chromatography gave the compound **13** in 90% yield (210 mg). R_f = 0.2 in 100% EtOAc.

^{1}H NMR (400 MHz, $CDCl_3$): δ 6.83 (d, *J* = 8.0 Hz, 1H), 6.78 (s, 1H), 6.72 (d, *J* = 8.0 Hz, 1H), 5.90 (s, 1H), 4.31 (d, *J* = 5.6 Hz, 2H), 3.85 (s, 3H), 3.60 (t, *J* = 12.8 Hz, 2H), 2.18 (t, *J* = 7.6 Hz, 2H), 1.63-1.68 (m, 2H), 1.52-1.59 (m, 3H), 1.36-1.42 (3H) ppm. **^{13}C NMR (100 MHz, $CDCl_3$)**: δ 172.9, 146.7, 145.1, 130.2, 120.7, 114.4, 110.7, 62.4, 55.9, 43.5, 36.5, 32.2, 29.6, 29.3, 25.3, 25.2 ppm. **HRMS (ESI)** calcd for $C_{14}H_{21}NO_4$+H 268.1549, found 268.1543.

10-hydroxy-*N*-(4-hydroxy-3-methoxybenzyl)decanamide (14):

To a stirred solution of compound **12** (400 mg, 0.5472 mmol), in dry THF (10 mL) was added TBAF 1M in THF (0.87 mmol, 0.9 mL) at 0 ^{o}C, then stirring was continued for 4 h at rt, after 4h quenched with saturated ammonium chloride solution, extracted with ethyl acetate, finally with brine, dried and evaporated provided the crude product which was purified by column chromatography gave the compound **14** in 90% yield (210 mg). R_f = 0.36 in 70% EtOAc/Hexane.

^{1}H NMR (400 MHz, $CDCl_3$): δ 6.82 (d, *J* = 8.0 Hz, 1H), 6.78 (d, *J* = 1.6 Hz, 1H), 6.72 (dd, *J* = 1.6 Hz, *J* = 8.0 Hz, 1H), 5.91 (s, 1H), 4.32 (d, *J* = 5.6 Hz, 2H), 3.85 (s, 3H), 3.59 (t, *J* = 6.4 Hz, 2H), 2.16 (t, *J* = 7.6 Hz, 2H), 1.60 (t, *J* = 6.8 Hz, 2H), 1.51 (t, *J* = 7.2 Hz, 2H), 1.23 (s, 12H) ppm. **^{13}C NMR (100 MHz, $CDCl_3$)**: δ 173.1, 146.7, 145.1, 130.3, 120.7, 114.4, 110.7, 62.9, 55.9, 43.5, 36.7, 32.6, 29.6, 29.3, 29.2, 29.2, 25.7, 25.6 ppm. **HRMS (ESI)** calcd for $C_{18}H_{29}NO_4$+H 322.2175, found 324.2166.

***N*-(4-((*tert*-butyldimethylsilyl)oxy)-3-methoxybenzyl)-6-hydroxyhexanamide (15)**:

To a stirred solution of compound **11** (700 mg, 1.41 mmol) in acetonitrile (15 mL) was added $CeCl_3.7H_2O$ (1.0 g mg, 2.82 mmol) at room temperature, heated to reflux until completion of the reaction, after completion of the reaction, reaction mixture was partitioned between ethyl acetate and water, water layer was washed 2 times with ethyl acetate, the combined organic layer was washed with brine, dried over anhydrous sodium sulphate, filter and evaporation provided the crude product which was purified by silica-gel column chromatography gave the compound **15** in 80% yield (430 mg). R_f = 0. 45 in 70% EOAc/Hexane.

^{1}H NMR (400 MHz, $CDCl_3$): δ 6.75-6.78 (m, 2H), 6.68 (dd, *J* = 1.6 Hz, *J* = 8.0 Hz, 1H), 5.91 (s, 1H), 4.32 (d, *J* = 5.6 Hz, 2H), 3.77 (s, 3H), 3.60 (t, *J* = 6.4 Hz, 2H), 2.19 (t, *J* = 7.2 Hz, 2H), 2.03 (s, 2H), 1.63-1.71 (m, 2H), 1.52-1.58 (m, 2H), 1.35-1.45 (m, 2H), 1.25 (s, 2H), 0.98 (s, 9H), 0.13 (s, 6H) ppm. **^{13}C NMR (100 MHz, $CDCl_3$)**: δ 172.8, 151.0, 144.4, 131.7, 120.8, 120.1, 111.9, 62.4, 55.5, 43.4, 36.5, 32.2, 29.6, 25.7, 25.3, 25.3, 18.4, -4.6 ppm.

***N*-(4-((*tert*-butyldimethylsilyl)oxy)-3-methoxybenzyl)-10-hydroxydecanamide (16)**:

To a stirred solution of compound **12** (700 mg, 1.27 mmol) in acetonitrile (15 mL) was added $CeCl_3.7H_2O$ (945 mg, 2.54 mmol) at room temperature, heated to reflux until completion of the reaction, after completion of the reaction, reaction mixture was partitioned between ethyl acetate and water, water layer was washed 2 times with ethyl acetate, the combined organic layer was washed with brine, dried over anhydrous sodium sulphate, filter and evaporation provided the crude product which was purified by silica-gel column chromatography gave the compound **16** in 81% yield (450 mg). R_f = 0. 35 in 60% EOAc/Hexane.

^{1}H NMR (400 MHz, $CDCl_3$): δ 6.72 (d, *J* = 8.4 Hz, 2H), 6.64 (d, *J* = 7.6 Hz, 1H), 4.28 (d, *J* = 5.6 Hz, 2H), 3.73 (s, 3H), 3.52 (t, *J* = 6.4 Hz, 2H), 2.80 (bs, 1H), 2.13 (t, *J* = 7.6 Hz, 2H), 1.59 (bs, 2H), 1.47 (d, *J* = 6.4 Hz, 2H), 1.22 (s, 12H), 0.95 (s, 9H), 0.10 (s, 6H) ppm. **^{13}C NMR (100 MHz, $CDCl_3$)**: δ 173.2, 150.9, 144.3, 131.9, 120.7, 120.0, 111.8, 62.6, 55.4, 43.3, 36.6, 32.6, 29.4, 29.3, 29.2, 25.7, 18.4, -4.6 ppm.

***N*-(4-((*tert*-butyldimethylsilyl)oxy)-3-methoxybenzyl)-6-oxohexanamide (17)**:

To a stirred solution of compound **15** (400 mg, 1.05 mmol) in dry CH_2Cl_2 (10 mL) was added pyridinium dichromate (293 mg, 0.78 mmol) followed by acetic anhydride (3.57 mmol, 357 µL) at 0 ^oC, then stirring was continued for 4 h at 50 ^oC, after 4h cooled to room temperature, evaporation of the solvent followed by column chromatography provided the compound **17** in 83% yield (330 mg). R_f = 0.4 in 60% EtOAc/Hexane.

^{1}H NMR (400 MHz, $CDCl_3$): δ 9.73 (t, *J* = 2.4 Hz, 1H), 6.76 (d, *J* = 6.4 Hz, 1H), 6.74 (d, *J* = 1.6 Hz, 1H), 6.68 (dd, *J* = 1.6 Hz, *J* = 6.4 Hz, 1H), 5.88 (s, 1H), 4.32 (d, *J* = 4.4 Hz, 2H), 3.76 (s, 3H), 2.44 (dt, *J* = 1.2 Hz, *J* = 5.6 Hz, *J* = 11.2 Hz, 2H), 2.19 (t, J = 5.6 Hz, 2H), 1.62-1.69 (m, 5H), 0.97 (s, 9H), 0.12 (s, 6H) ppm. **^{13}C NMR (100 MHz, $CDCl_3$)**: δ 202.1, 172.1, 151.0, 144.5, 131.7, 120.8, 120.2, 112.0, 55.5, 43.5, 43.5, 36.2, 25.7, 25.0, 21.5, 18.4, -4.6 ppm.

***N*-(4-((*tert*-butyldimethylsilyl)oxy)-3-methoxybenzyl)-10-oxodecanamide (18)**:

To a stirred solution of compound **16** (400 mg, 0.91 mmol) in dry DCM (10 mL) was added pyridinium dichromate (253 mg, 0.67 mmol) followed by acetic anhydride (3.09 mmol, 310 µL) at 0 ^oC, then stirring was continued for 4 h at 50 ^oC, after 4h cooled to room temperature, evaporation of the solvent followed by column chromatography provided the compound **18** in 80% yield (270 mg). R_f = 0.53 in 30% EtOAc/Hexane.

^{1}H NMR (400 MHz, $CDCl_3$): δ 9.69 (s, 1H), 6.72 (d, *J* = 8.0 Hz, 2H), 6.64 (d, *J* = 8.0 Hz, 1H), 6.03 (s, 1H), 4.28 (d, *J* = 5.6 Hz, 2H), 3.73 (s, 3H), 2.34 (t, *J* = 7.2 Hz, 2H), 2.13 (t, *J* = 7.2 Hz, 2H), 1.56 (t, *J* = 6.4 Hz, 4H), 1.25 (s, 9H), 0.94 (s, 9H), 0.10 (s, 6H) ppm. **^{13}C NMR (100 MHz, $CDCl_3$)**: δ 202.9, 172.9, 150.9, 144.3, 131.9, 120.7, 120.0, 111.8, 55.4, 43.8, 43.3, 36.6, 29.1, 29.1, 29.0, 25.6, 21.9, 18.4, -4.6 ppm.

***N*-(4-((*tert*-butyldimethylsilyl)oxy)-3-methoxybenzyl)-6-oxohexanamide (19)**:

To a stirred solution of compound **17** (200 mg, 0.52 mmol), in dry THF (6 mL) was added TBAF 1M in THF (0.63 mmol, 0.63 mL) at 0 ^oC, then stirring was continued for 3 h at rt, after 3 h quenched with saturated ammonium chloride solution, extracted with ethyl acetate, finally with brine, dried and evaporated provided the crude product which was purified by column chromatography gave the compound **19** in 90% yield (125 mg). R_f = 0.38 in 100% EtOAc.

^{1}H NMR (400 MHz, $CDCl_3$): δ 9.75 (s, 1H), 6.84 (d, *J* = 8.0 Hz, 1H), 6.80 (s, 1H), 6.75 (d, *J* = 8.4 Hz, 1H), 5.80 (t, *J* = 3.6 Hz, 1H), 4.34 (d, *J* = 5.6 Hz, 2H), 3.87 (s, 3H), 2.46 (t, *J* = 6.8 Hz, 2H), 2.20 (t, *J* = 6.8 Hz, 2H), 1.66 (t, *J* = 2.8 Hz, 5H) ppm. **^{13}C NMR (100 MHz, $CDCl_3$)**: δ 202.2, 172.2, 146.7, 145.1, 130.1, 120.8, 114.4, 110.7, 55.9, 43.6, 36.3, 29.6, 25.0, 21.5 ppm. **HRMS (ESI)** calcd for $C_{14}H_{19}NO_4$+H 266.1392, found 266.1384.

***N*-(4-hydroxy-3-methoxybenzyl)-10-oxodecanamide (20)**:

To a stirred solution of compound **18** (200 mg, 0.54 mmol), in dry THF (6 mL) was added TBAF 1M in THF (0.65 mmol, 0.65 mL) at 0 ^oC, then stirring was continued for 3 h at rt, after 3h quenched with saturated ammonium chloride solution, extracted with ethyl acetate, finally with brine, dried and evaporated provided the crude product which was purified by column chromatography gave the compound **20** in 90% yield (160 mg). R_f = 0.36 in 60% EtOAc/Hexane.

^{1}H NMR (400 MHz, $CDCl_3$): δ 9.75 (s, 1H), 6.85 (d, *J* = 8.0 Hz, 1H), 6.80 (s, 1H), 6.75 (d, *J* = 8.0 Hz, 1H), 5.70 (s, 1H), 4.34 (d, *J* = 5.6 Hz, 2H), 3.87 (s, 3H), 2.39 (t, *J* = 7.2 Hz, 2H), 2.17 (t, *J* = 7.6 Hz, 2H), 1.61 (t, *J* = 6.4 Hz, 5H), 1.29 (s, 8H) ppm. **^{13}C NMR (100 MHz, $CDCl_3$)**: δ 203.0, 173.0, 146.8, 145.1, 130.2, 120.6, 114.4, 110.7, 55.8, 43.8, 43.4, 36.7, 29.6, 29.1, 29.0, 25.7, 21.9 ppm. **HRMS (ESI)** calcd for $C_{18}H_{27}NO_4$+H 322.2018, found 322.22010.

Literature Cited

1. Gannett PM, Nagel DL, Reilly PJ, Lawson T, Sharpe J, Toth B 1988. The capsaicinoids: Their separation, synthesis, and mutagenicity. J Org Chem 53:1064-1071.

2. Ankala SV, Fenteany G 2002. Selective deprotection of either alkyl or aryl silyl ethers from aryl, alkyl bis-silyl ethers. Tetrahedron Lett 43:4729-4732.

^{1}H and ^{13}C NMR spectra of compounds

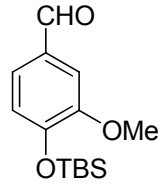

2

^{1}H-NMR, 400 MHz, $CDCl_3$

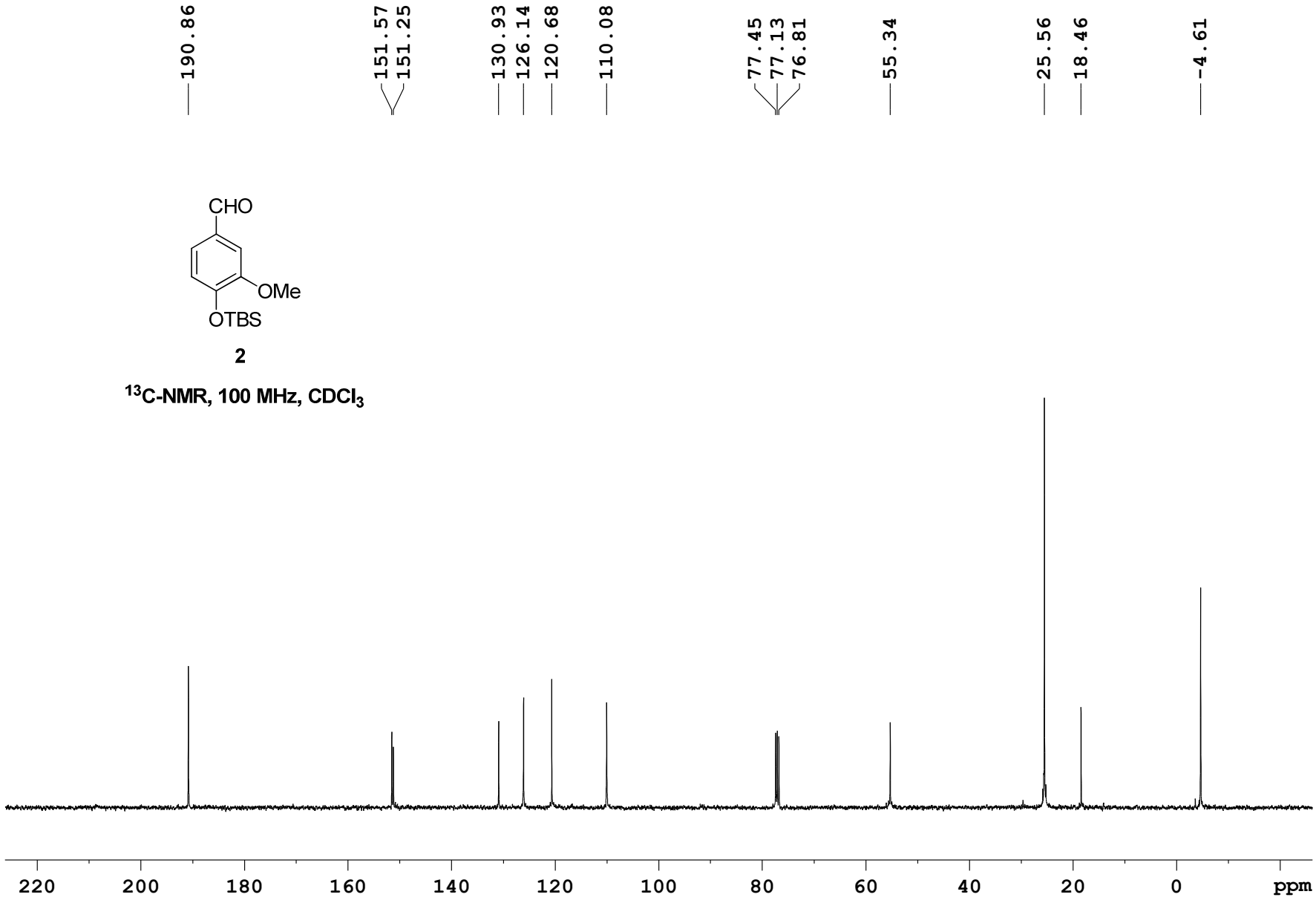

2

^{13}C-NMR, 100 MHz, $CDCl_3$

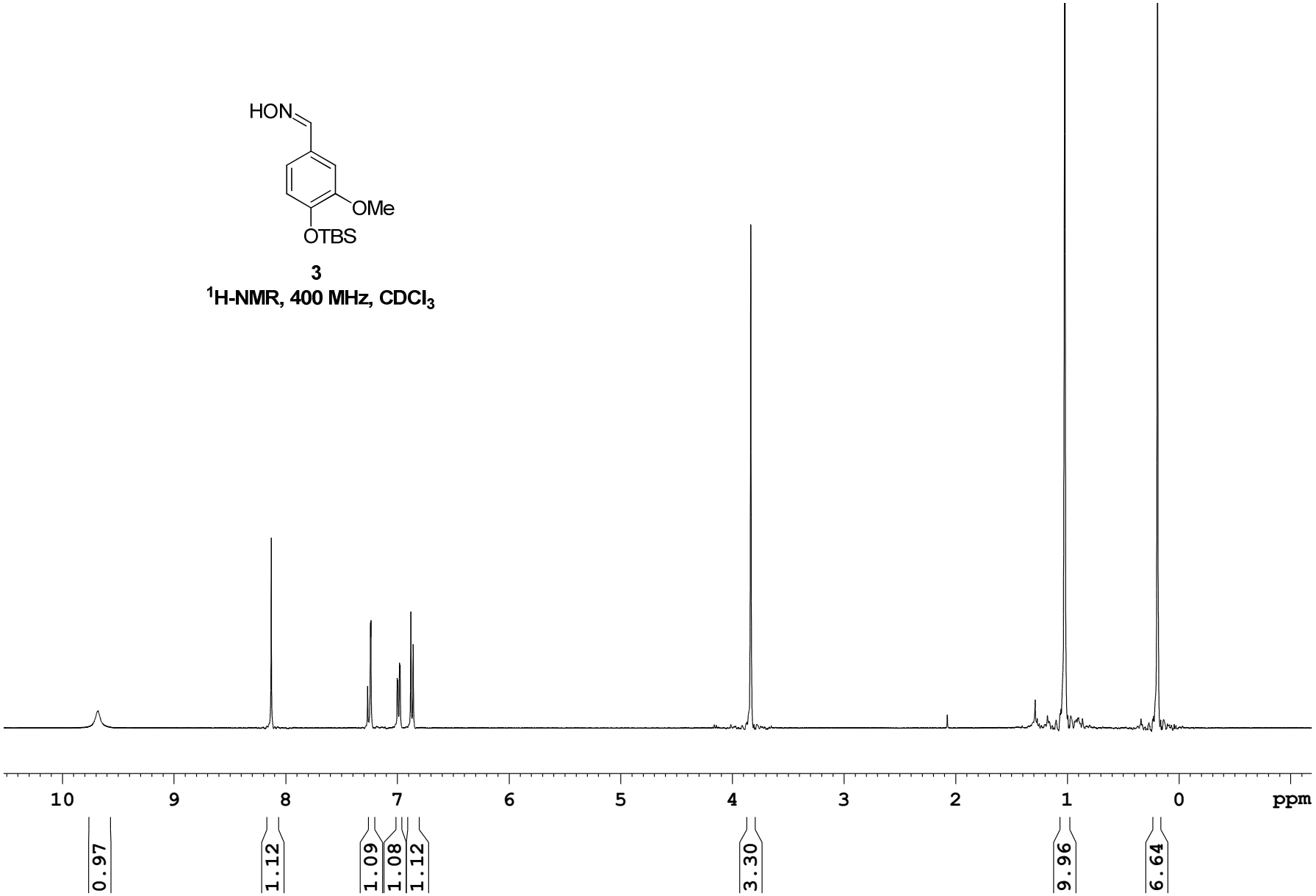
HON
OMe
OTBS
3
1H-NMR, 400 MHz, CDCl3
10
9
8
7
6
5
4
3
2
1
0
ppm
0.97
1.12
1.09
1.08
1.12
3.30
9.96
6.64

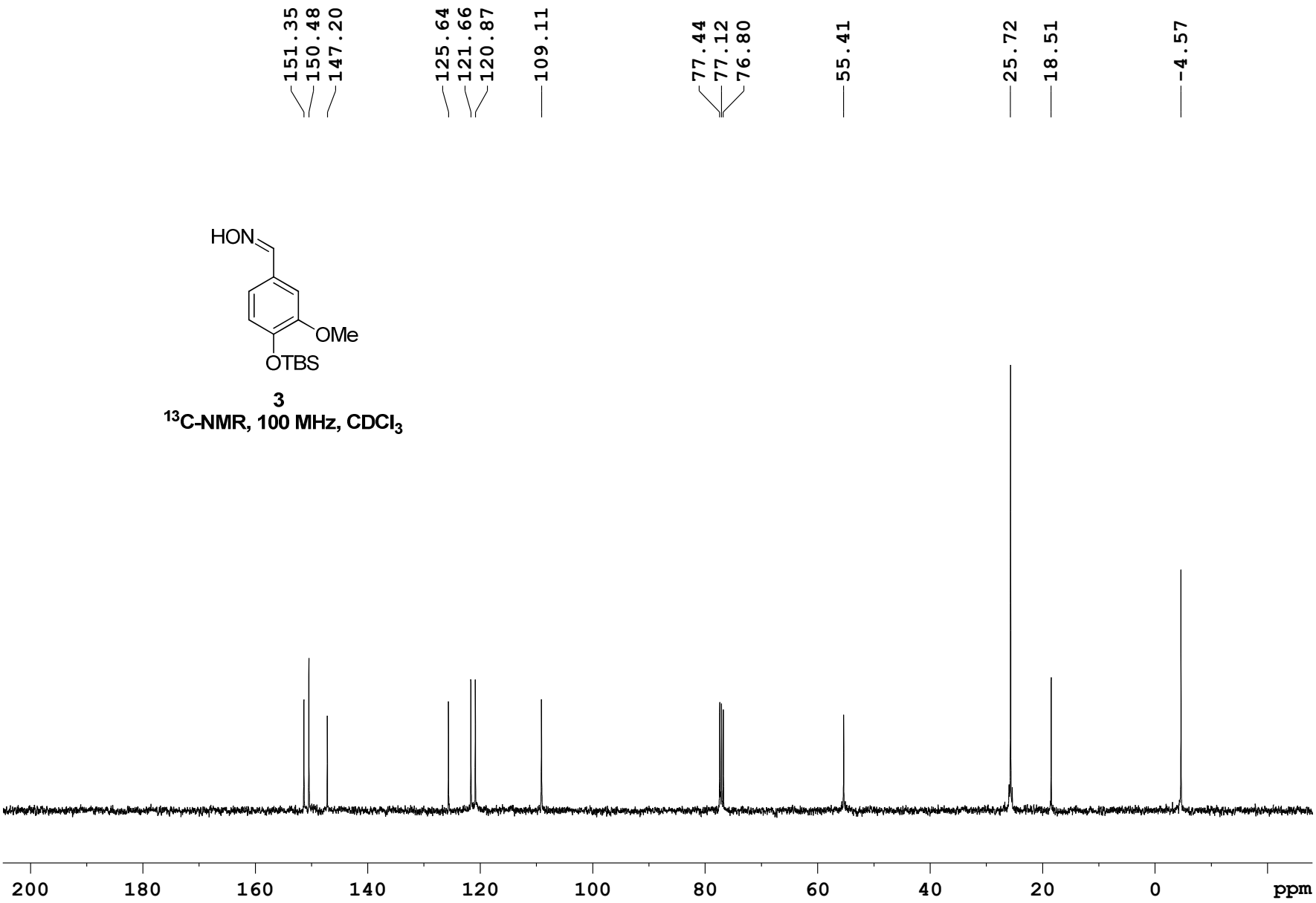

3

^{13}C-NMR, 100 MHz, $CDCl_3$

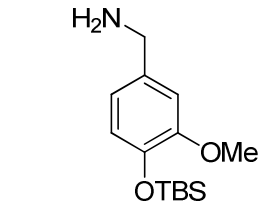

4

^{1}H-NMR, 400 MHz, $CDCl_3$

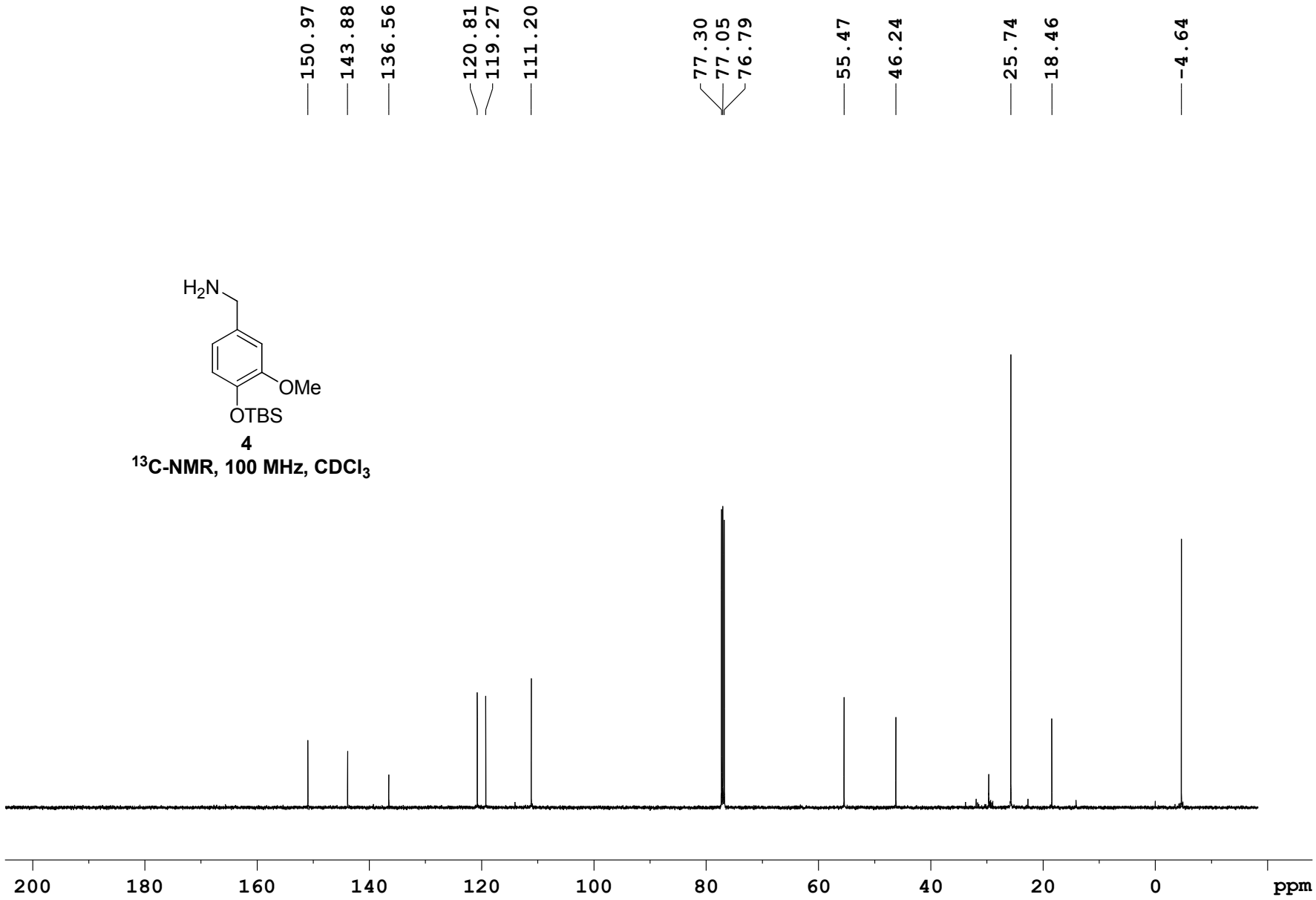

4

^{13}C-NMR, 100 MHz, $CDCl_3$

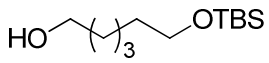

7

^{1}H-NMR, 400 MHz, $CDCl_3$

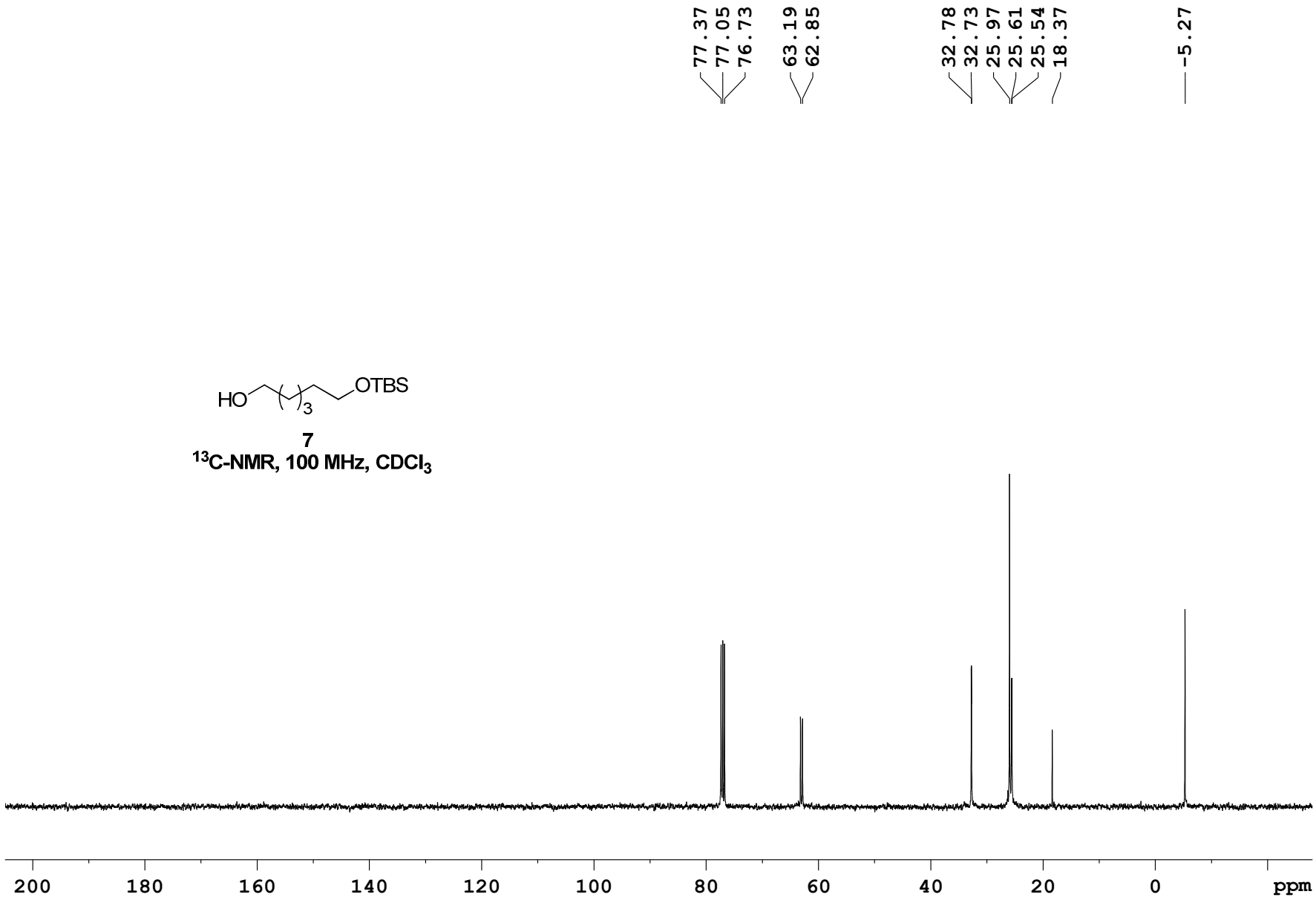
77.37
77.05
76.73
63.19
62.85
32.78
32.73
25.97
25.61
25.54
18.37
-5.27
HO
OTBS
3
7
13C-NMR, 100 MHz, CDCl3
200
180
160
140
120
100
80
60
40
20
0
ppm

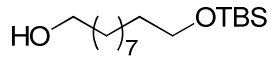

8

^{1}H-NMR, 500 MHz, $CDCl_3$

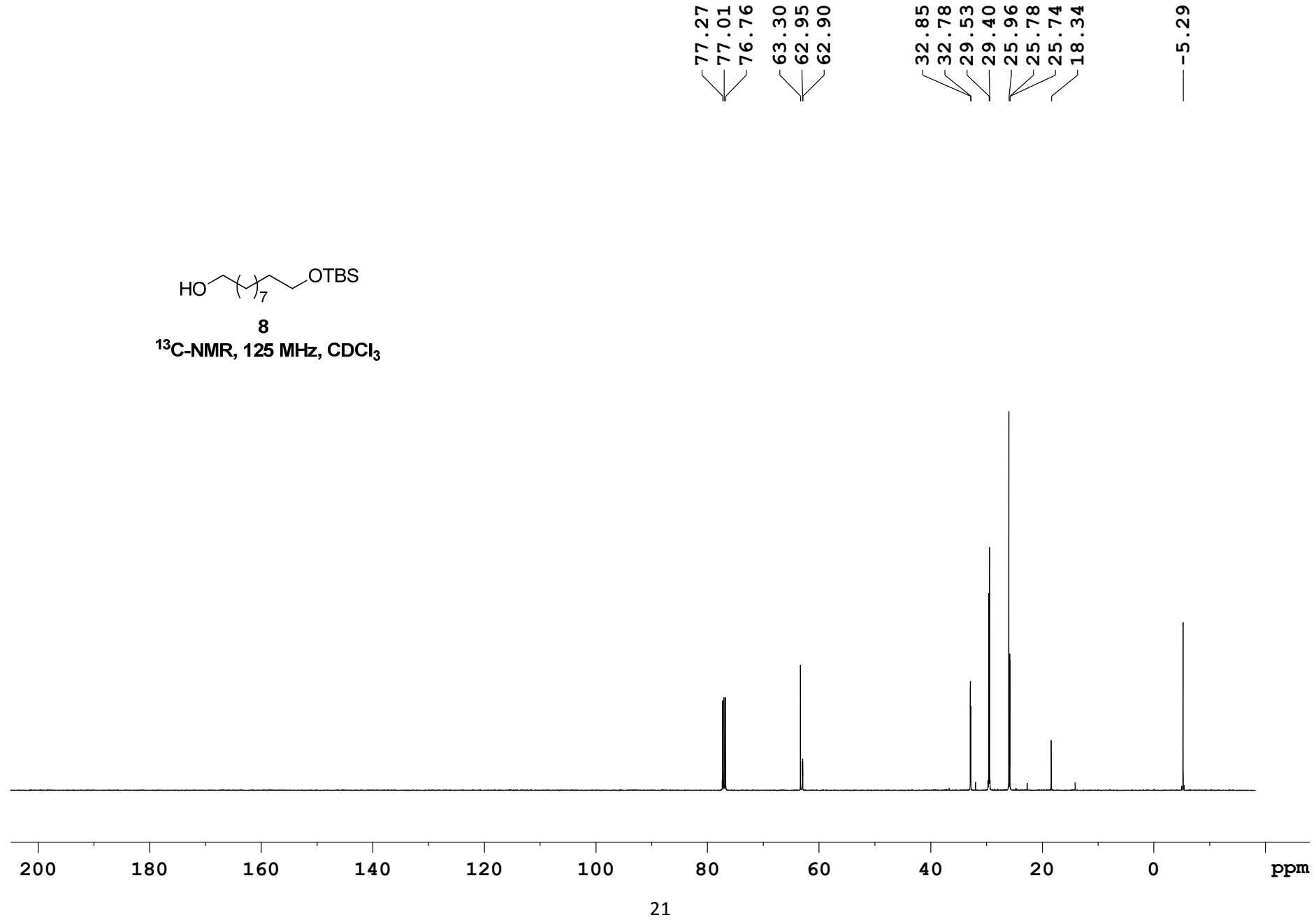

8

^{13}C-NMR, 125 MHz, $CDCl_3$

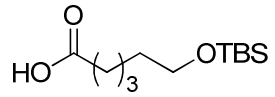

9

^{1}H-NMR, 400 MHz, $CDCl_3$

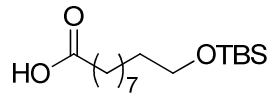

10

^{1}H-NMR, 400 MHz, $CDCl_3$

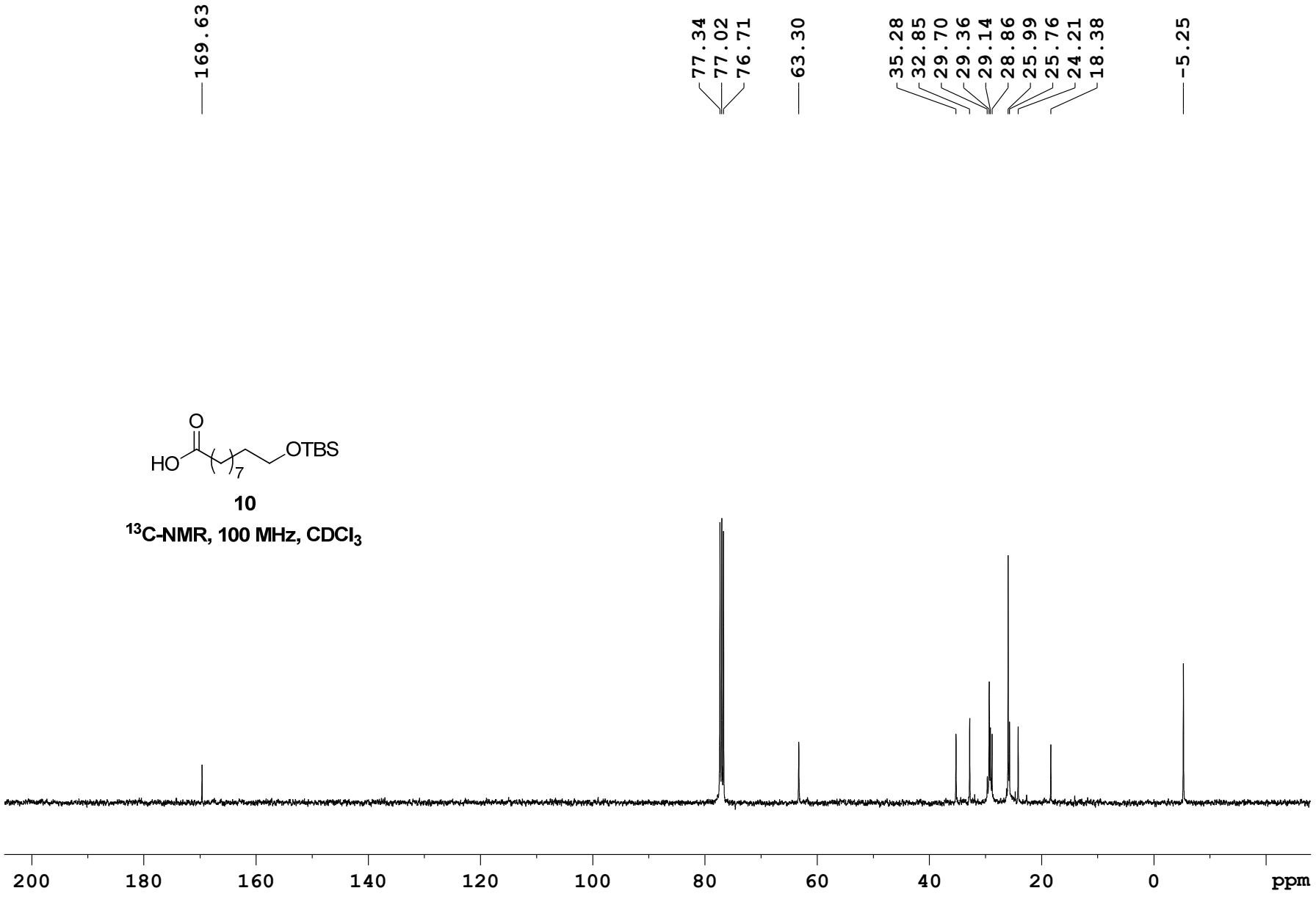

10

^{13}C-NMR, 100 MHz, $CDCl_3$

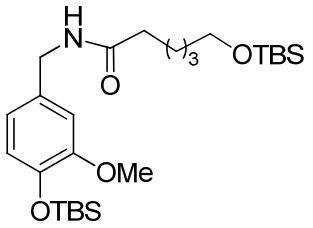

11

^{1}H-NMR, 400 MHz, $CDCl_3$

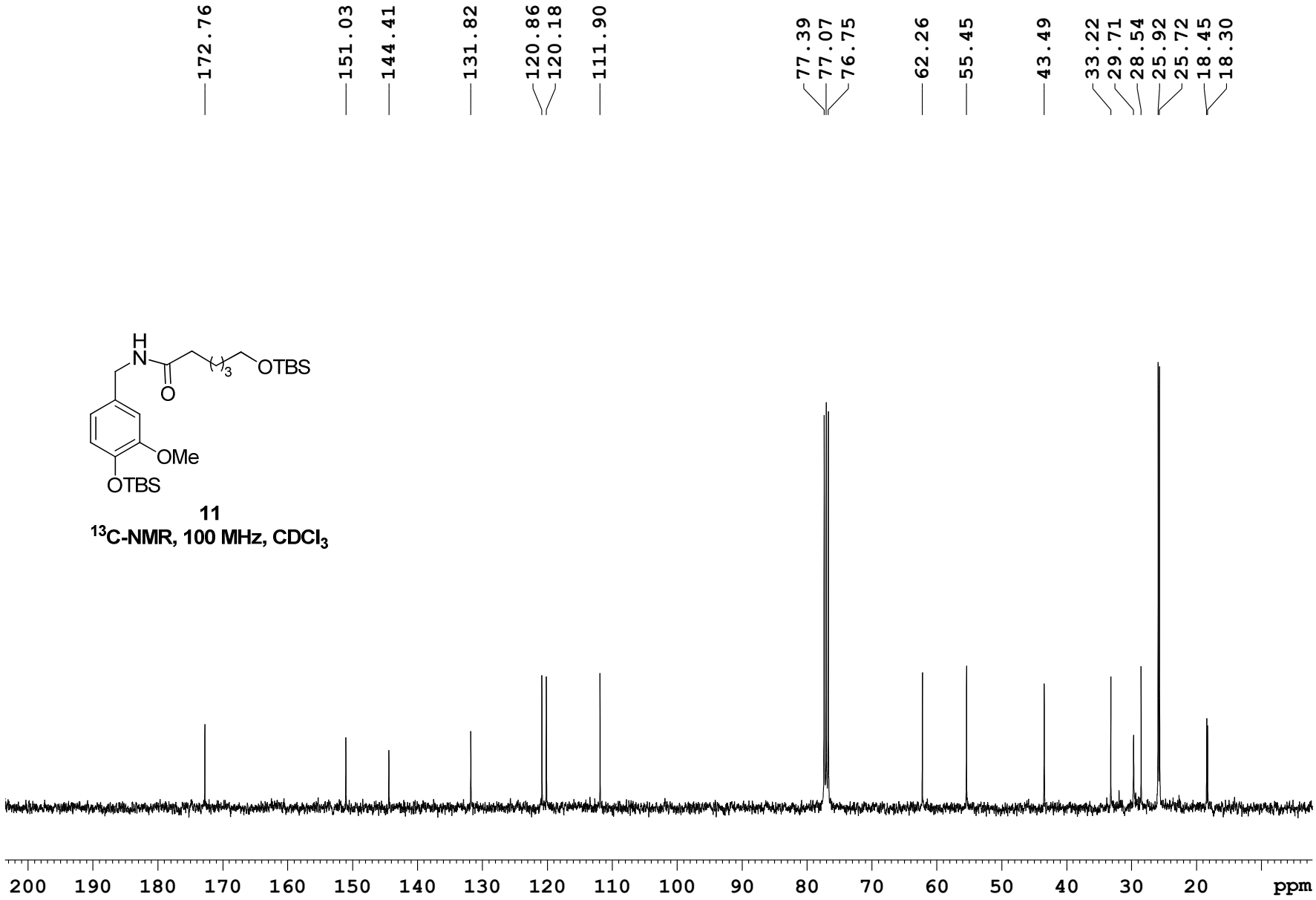

11

^{13}C-NMR, 100 MHz, $CDCl_3$

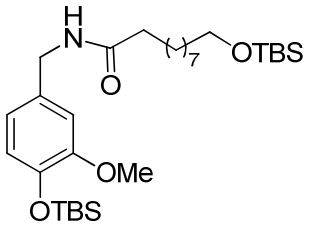

12

^{1}H-NMR, 400 MHz, $CDCl_3$

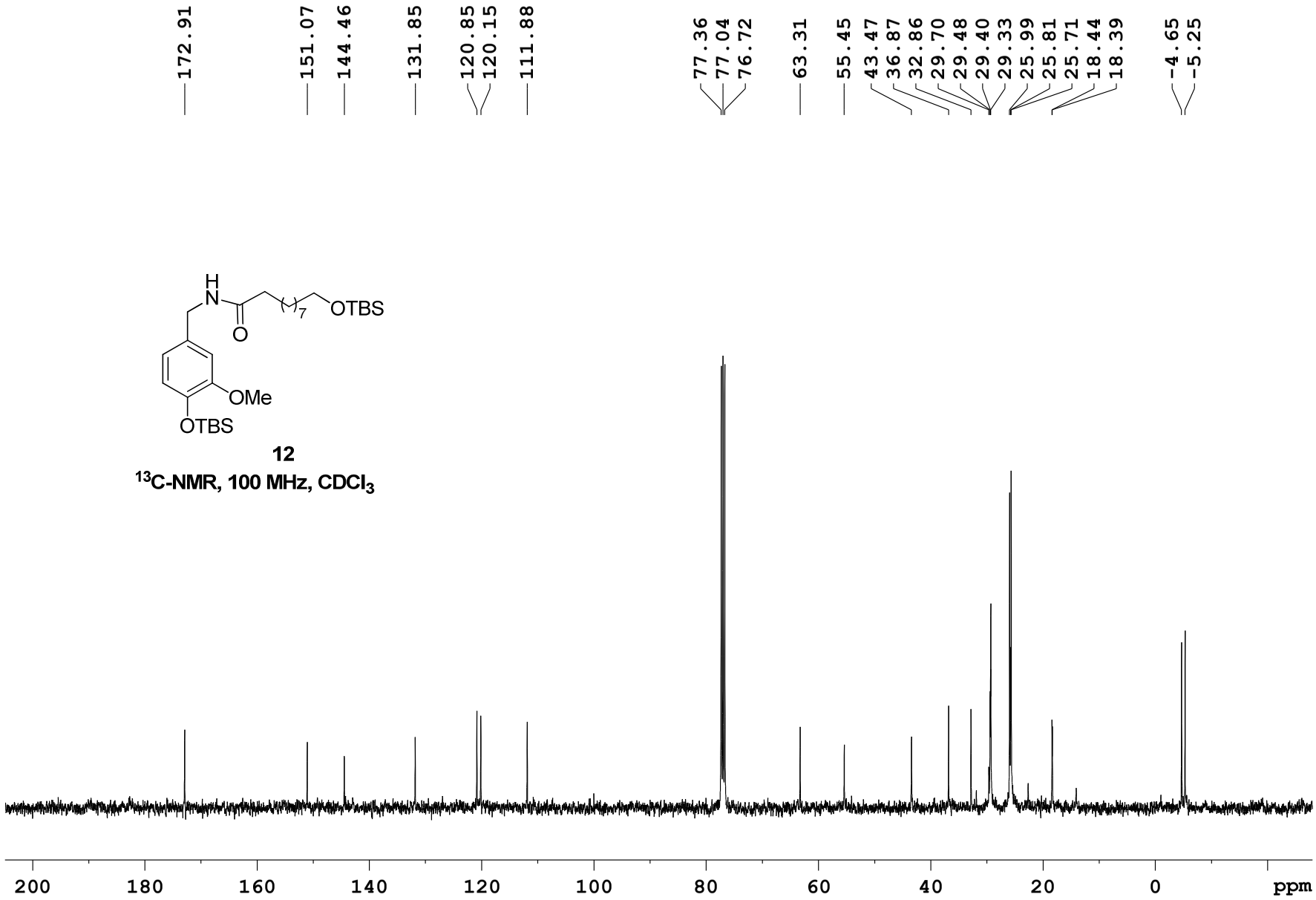

12

^{13}C-NMR, 100 MHz, $CDCl_3$

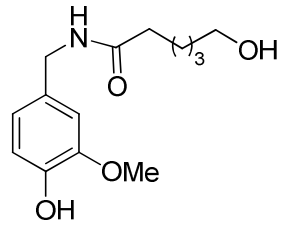

13

^{1}H-NMR, 400 MHz, $CDCl_3$

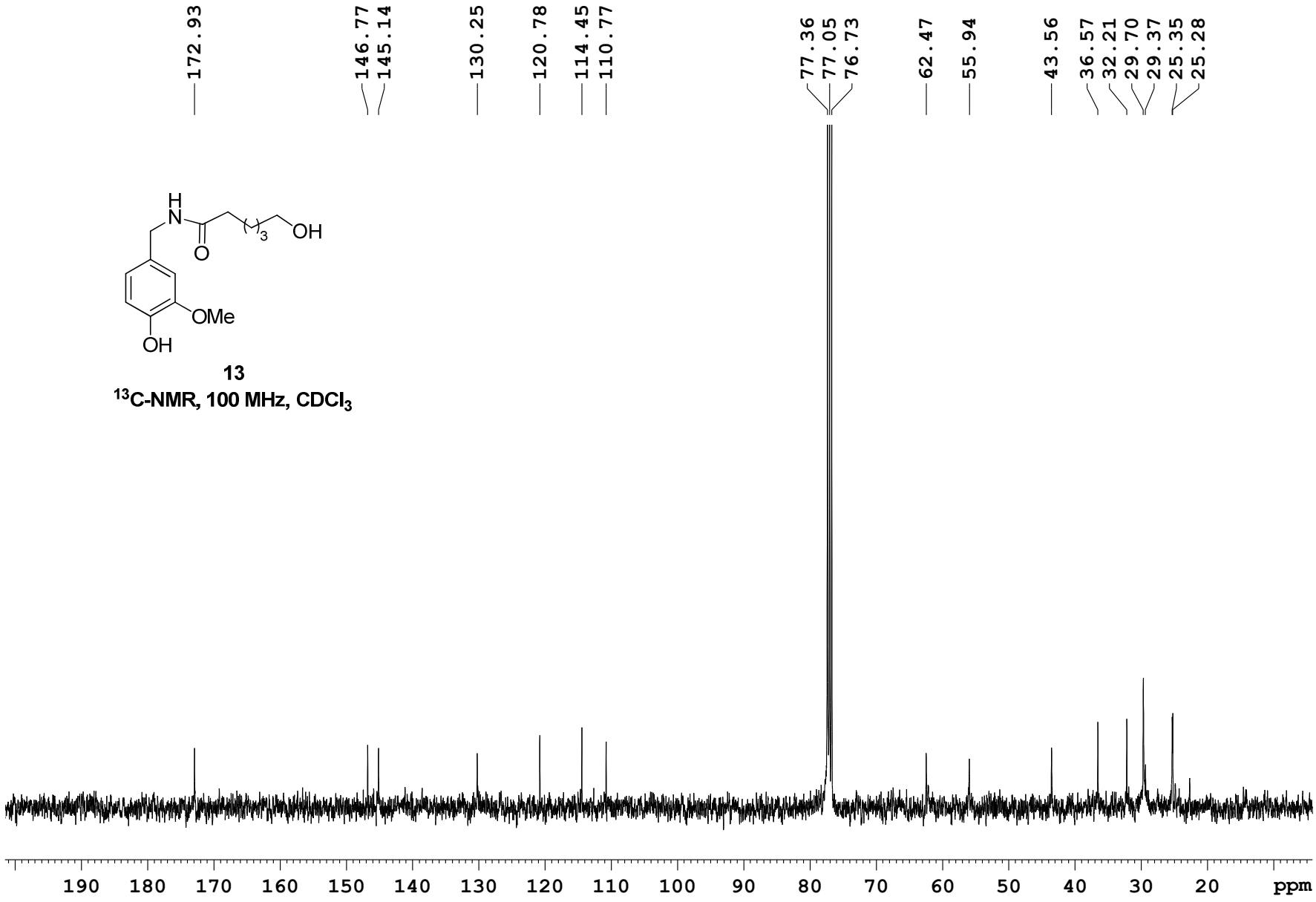

13

^{13}C-NMR, 100 MHz, $CDCl_3$

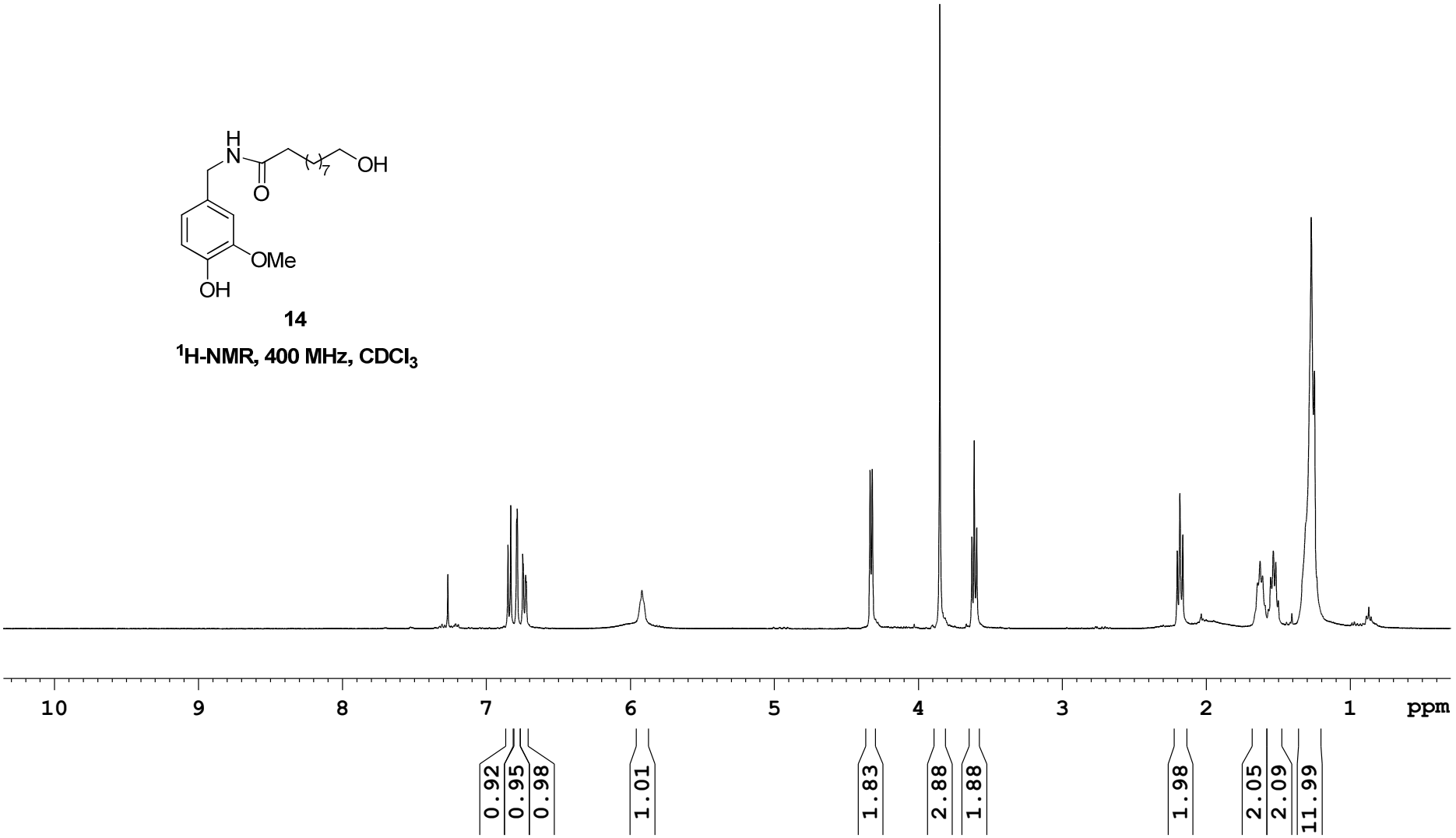
H
N
O
7
OH
OMe
OH
14
1H-NMR, 400 MHz, CDCl3
10
9
8
7
6
5
4
3
2
1
ppm
0.92
0.95
0.98
1.01
1.83
2.88
1.88
1.98
2.05
2.09
11.99

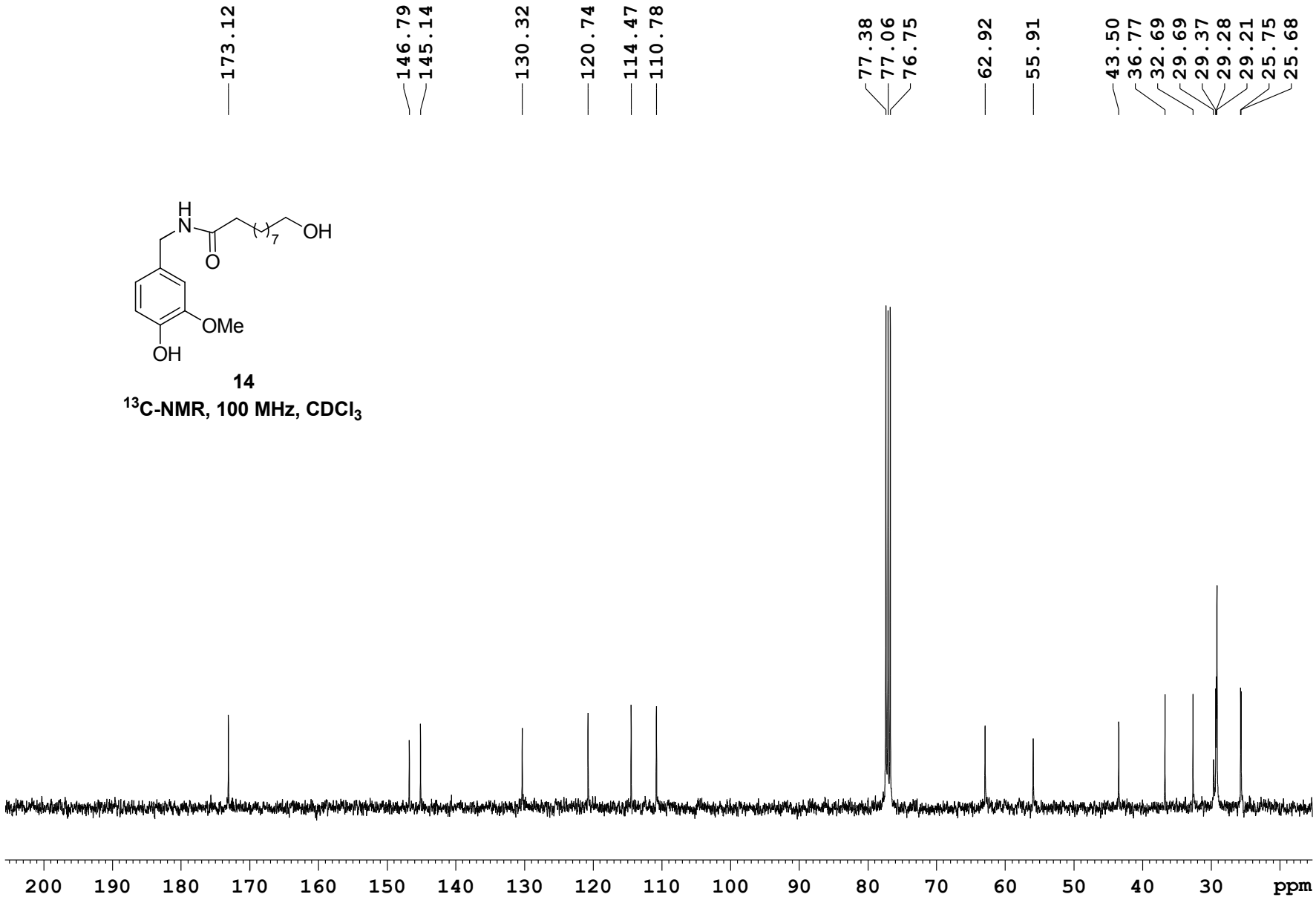

14

^{13}C-NMR, 100 MHz, $CDCl_3$

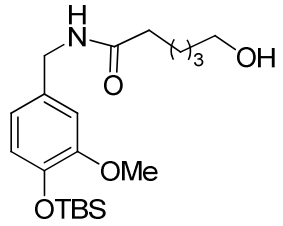

15

^{1}H-NMR, 400 MHz, $CDCl_3$

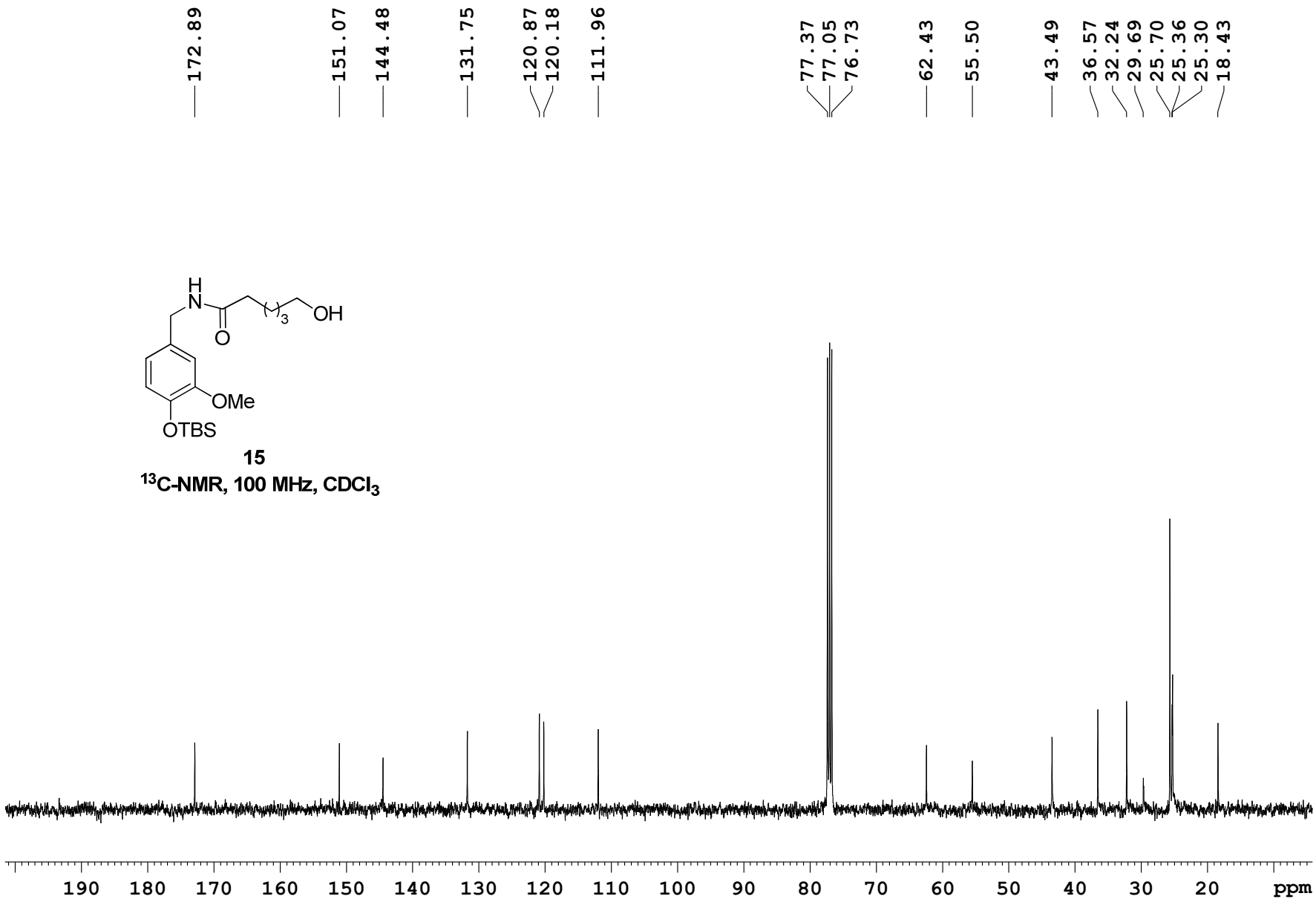

15

^{13}C-NMR, 100 MHz, $CDCl_3$

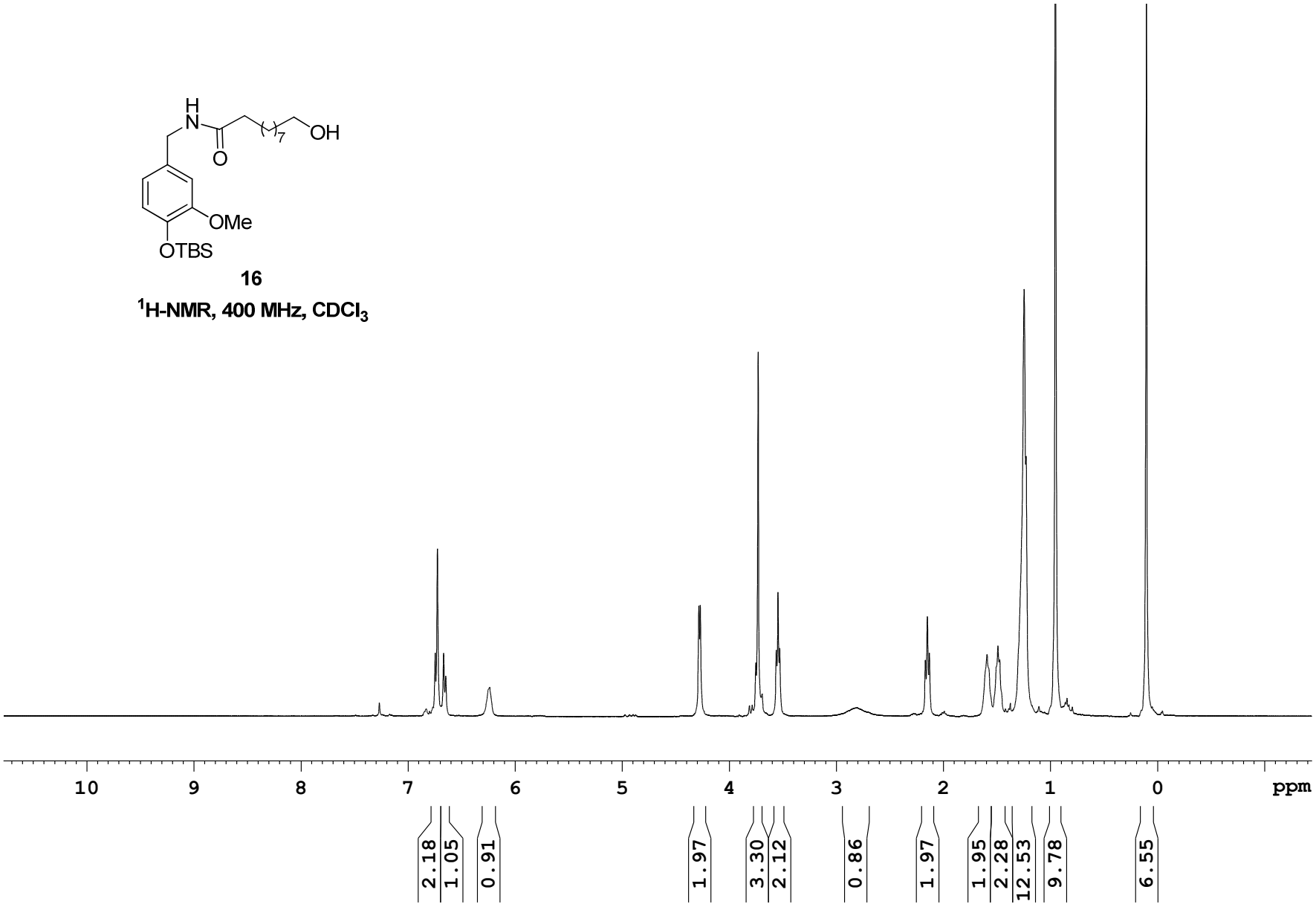
H
N
O
OH
OMe
OTBS
16
1H-NMR, 400 MHz, CDCl3
10
9
8
7
6
5
4
3
2
1
0
ppm
2.18
1.05
0.91
1.97
3.30
2.12
0.86
1.97
1.95
2.28
12.53
9.78
6.55

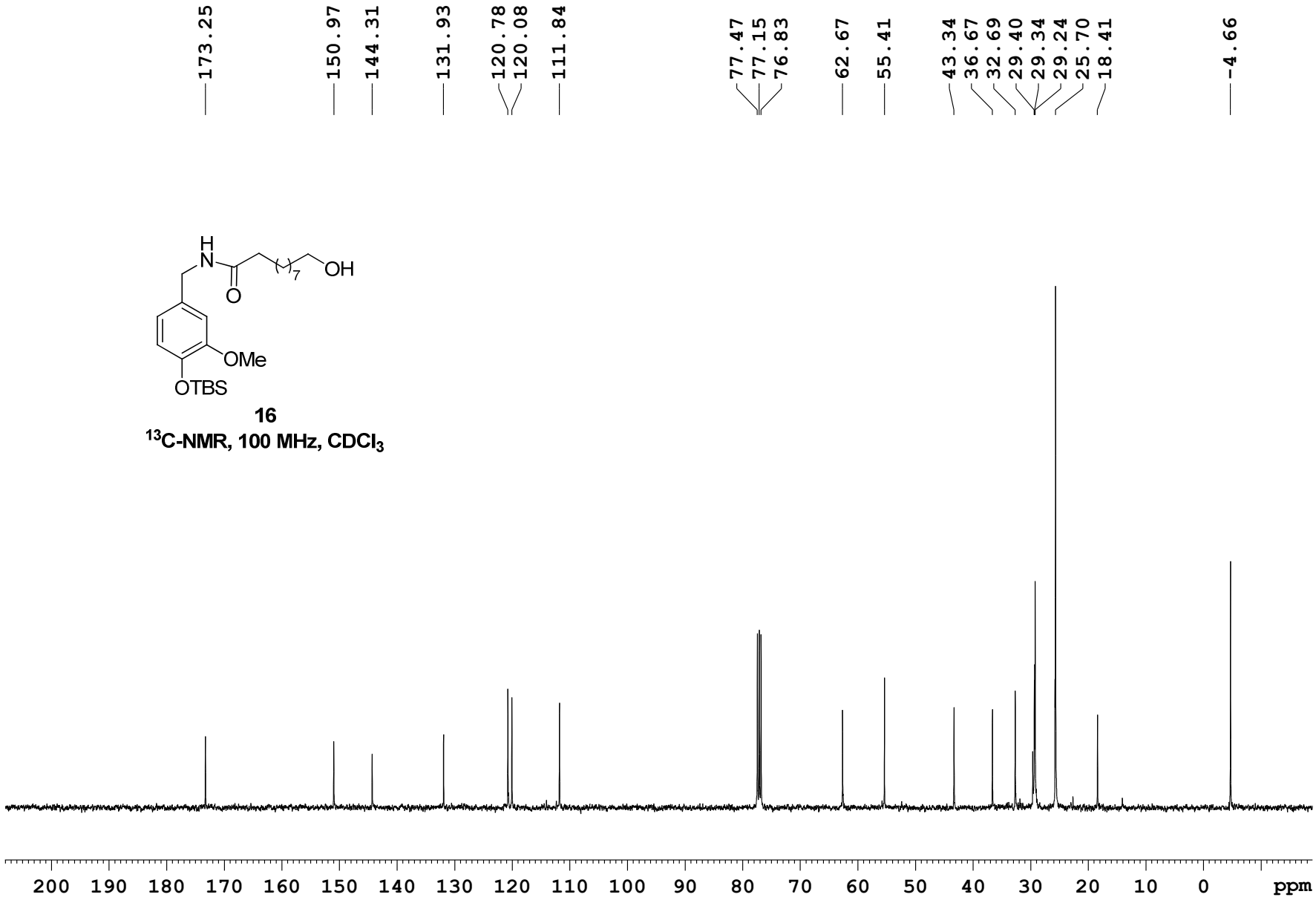

16

^{13}C-NMR, 100 MHz, $CDCl_3$

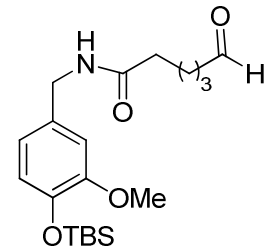

17

^{1}H-NMR, 400 MHz, $CDCl_3$

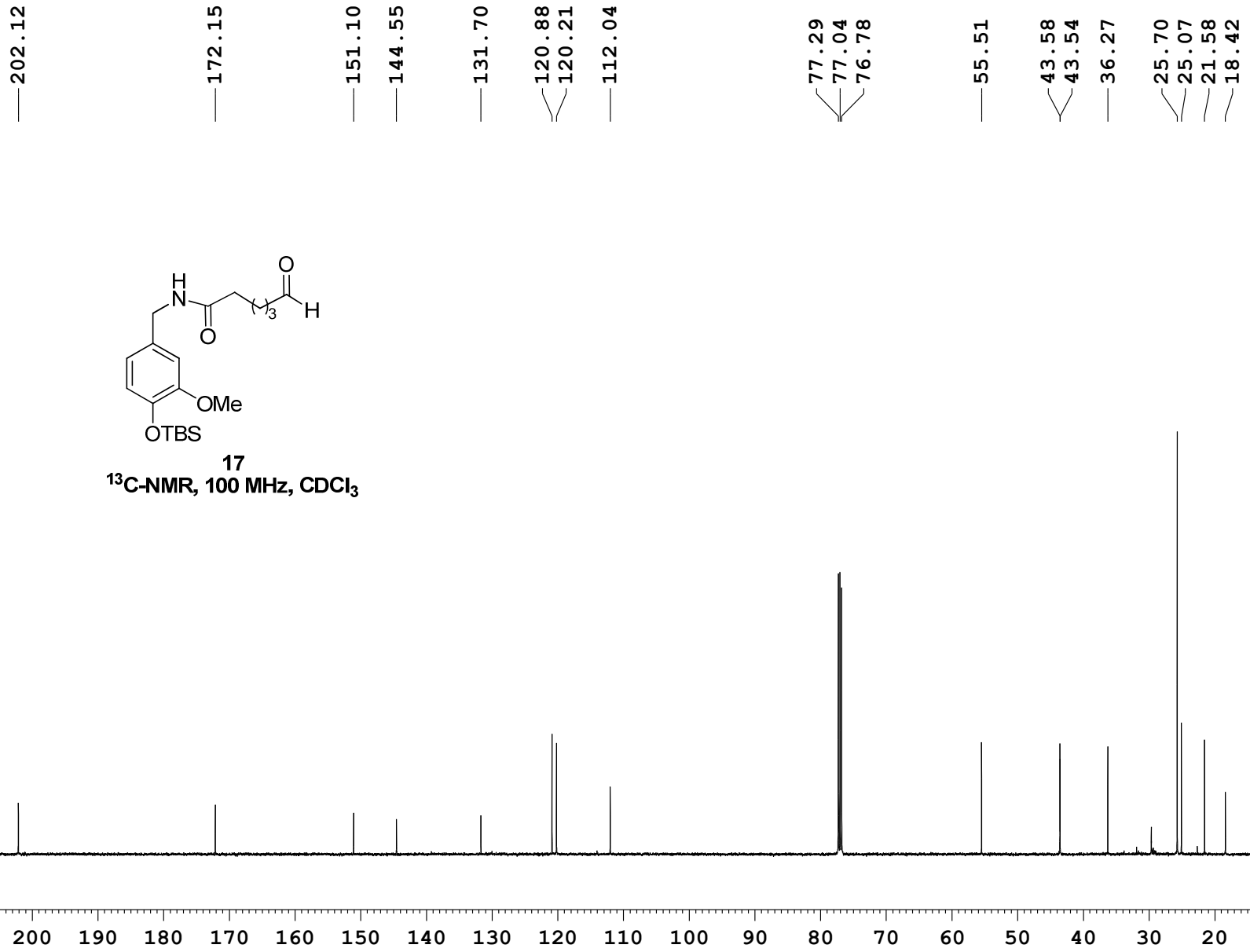

17

^{13}C-NMR, 100 MHz, $CDCl_3$

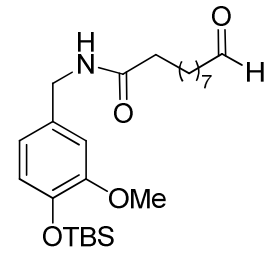

18

^{1}H-NMR, 400 MHz, $CDCl_3$

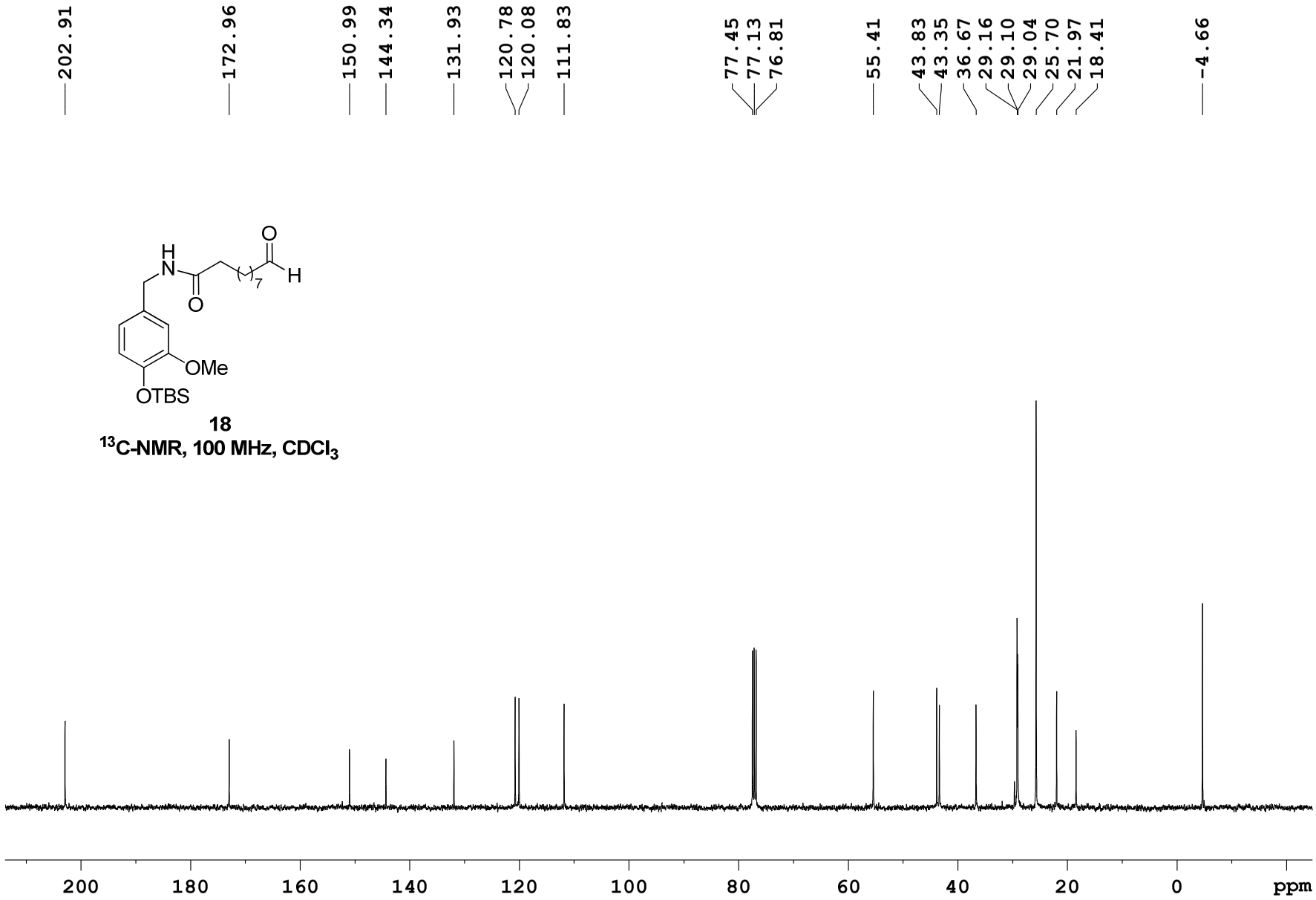

18

^{13}C-NMR, 100 MHz, $CDCl_3$

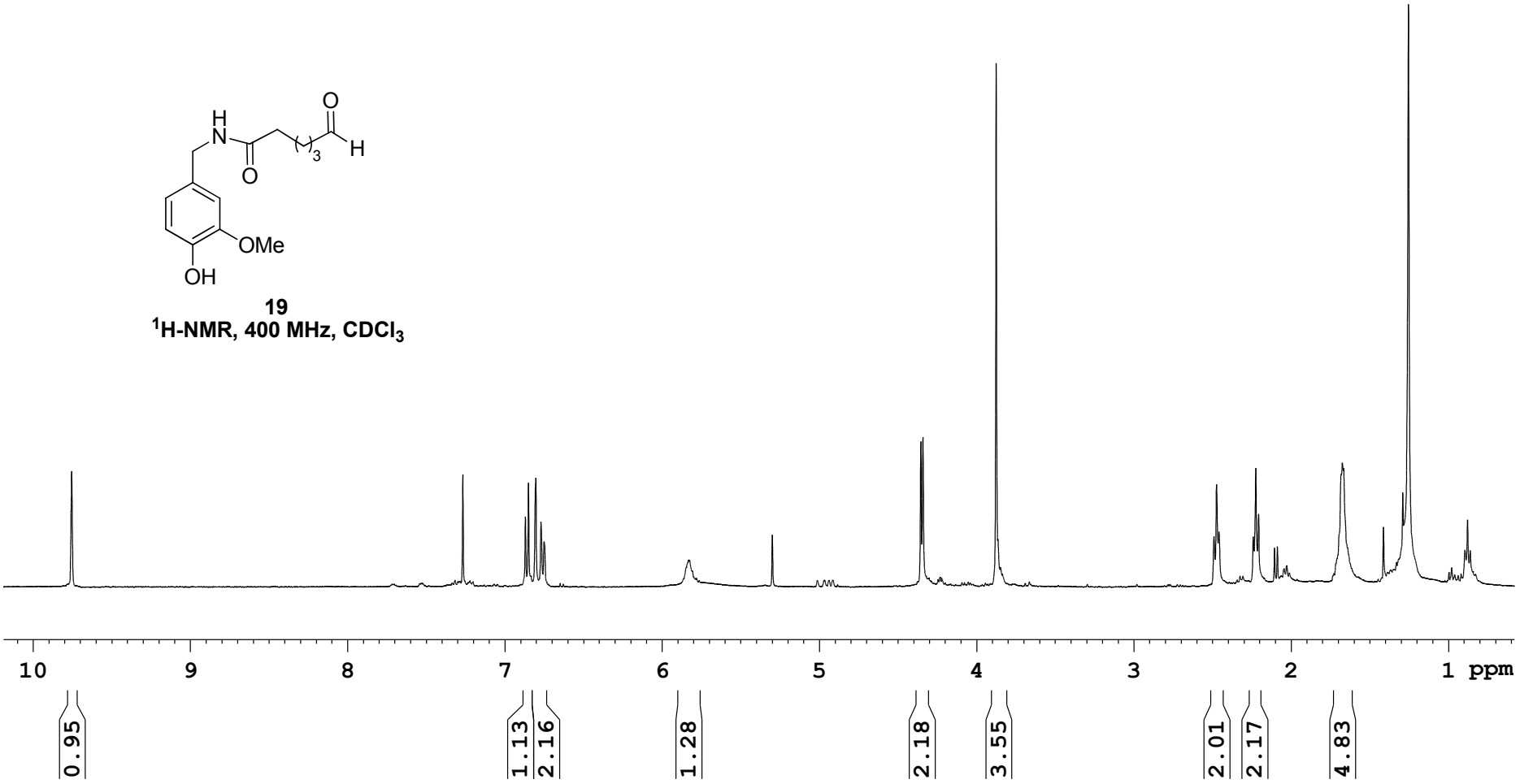

19

^{1}H-NMR, 400 MHz, $CDCl_3$

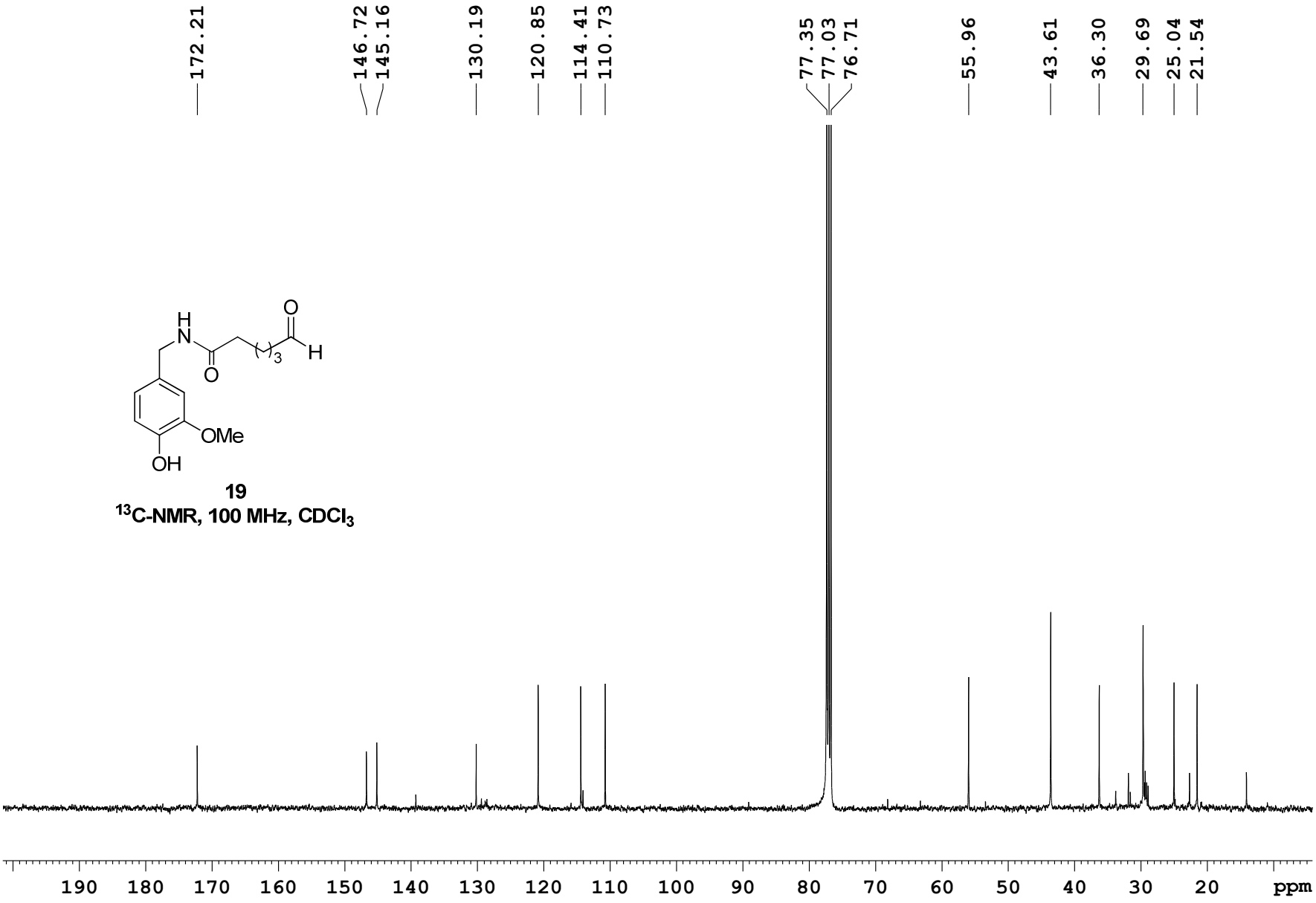
172.21
146.72
145.16
130.19
120.85
114.41
110.73
77.35
77.03
76.71
55.96
43.61
36.30
29.69
25.04
21.54
H
N
O
O
3
H
OMe
OH
19
13C-NMR, 100 MHz, CDCl3
190
180
170
160
150
140
130
120
110
100
90
80
70
60
50
40
30
20
ppm

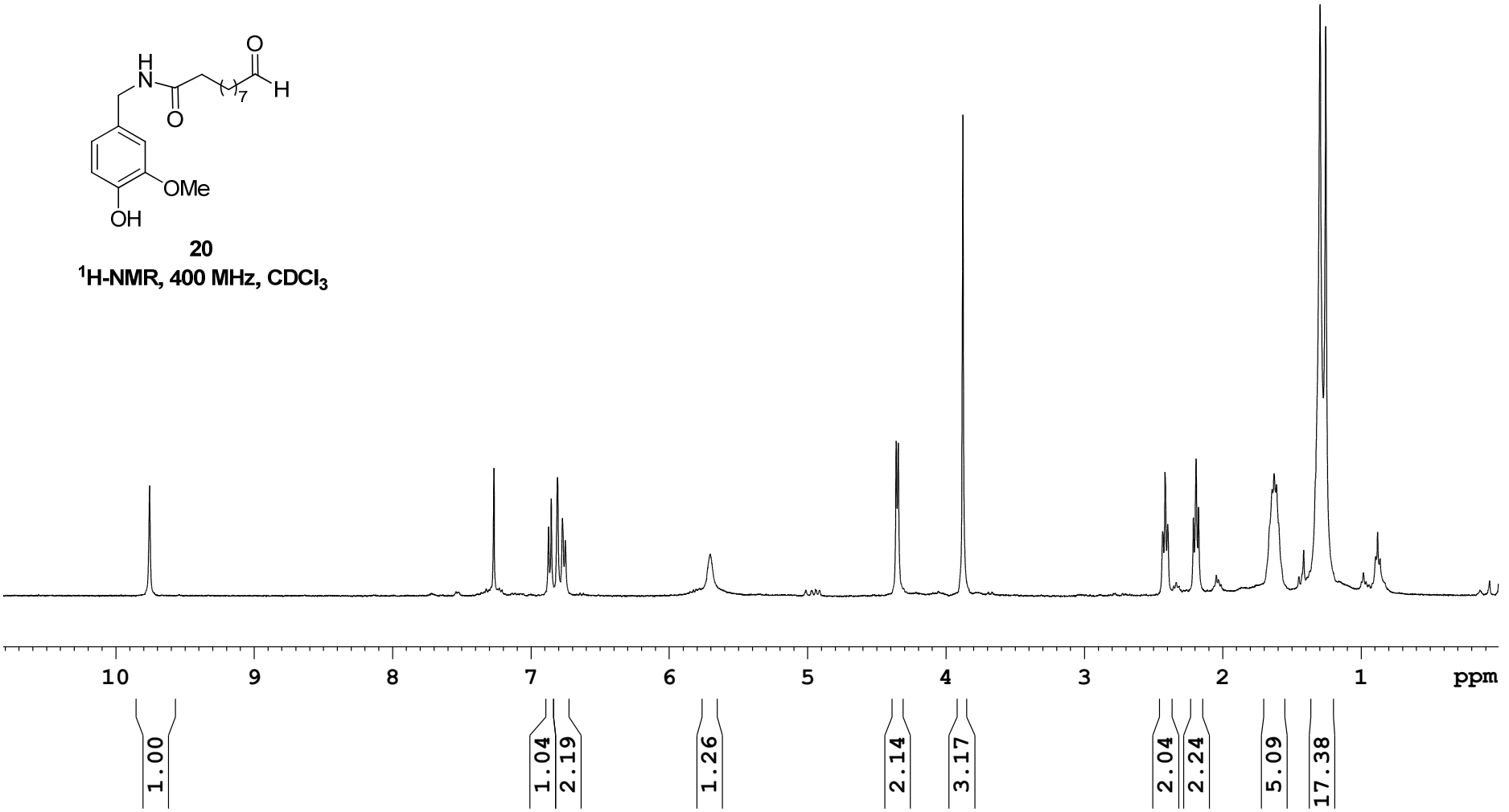

20

^{1}H-NMR, 400 MHz, $CDCl_3$

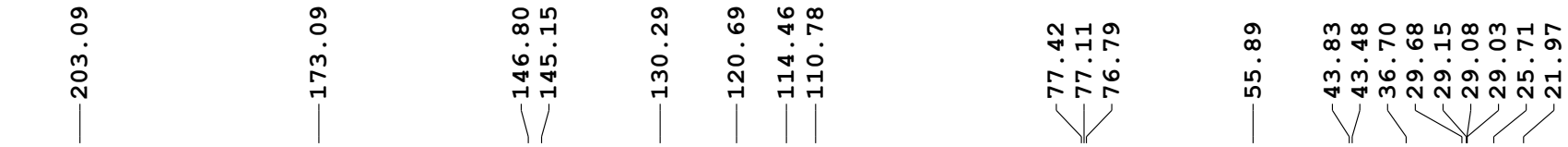

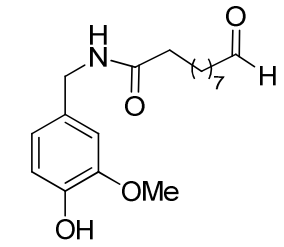

20

^{13}C-NMR, 100 MHz, $CDCl_3$

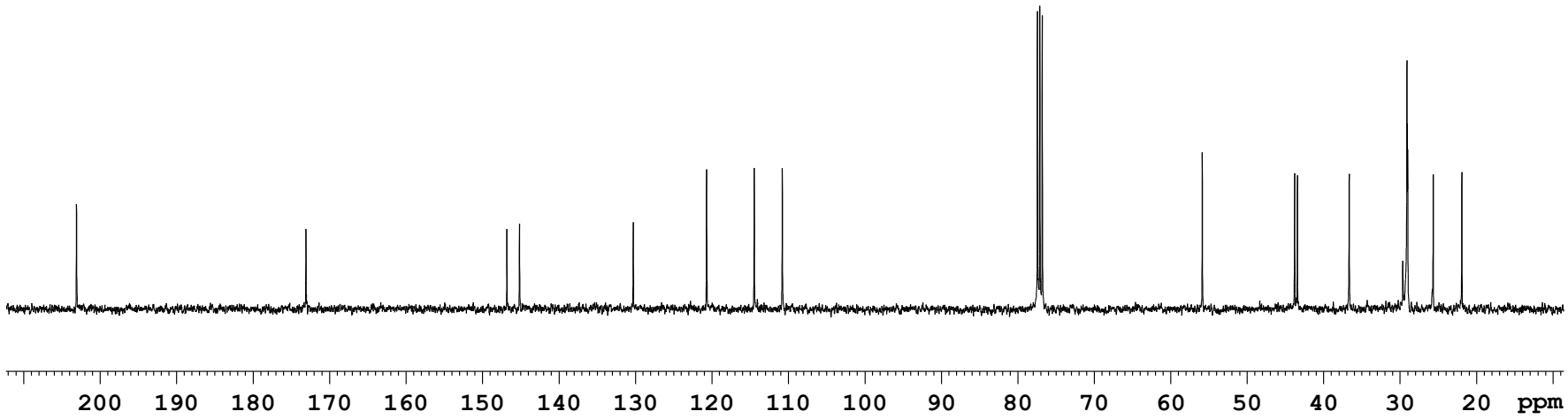

RNA Isolation and PCR

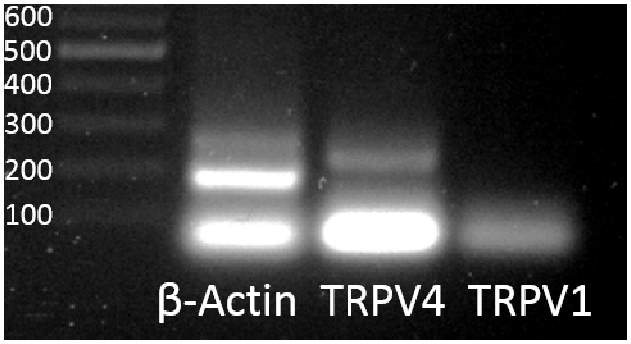

TRPV-1 canis: 559 bp
TRPV-4 canis: 237 bp
β-Actin canis: 130 bp

PCR products in a 1% w/v agarose gel. While the bands for β-actin and TRPV4 are visible a band for TRPV1 was not observed.

Total RNA was extracted using the RNeasy mini kit (Qiagen, Hilden, Germany), following the manufacturer's protocol. The cDNAs were synthesized with the reverse transcription system (Promega, Madison, USA) from 1 µg of total RNA per sample by following the manufacturer's instructions. The PCR primer sets were designed as follows: TRPV1 canis Forward: 5'-CCCCTGGATGGAGACCCTAA -3' and Reverse, 5'- ATGGCAATATGCAGGGCTG -3'; TRPV4 canis Forward, 5'- GATCGGGGTCTTTCAGCACA -3' and Reverse, 5'-TCCCGCAGCAGTTCATTGAT -3'; β-actin canis Forward, 5'- CAAAGCCAACCGTGAGAAG -3' and Reverse, 5'- CAGAGTCCATGACAATACCAG -3'. The primer sets were purchased from Eurofins MWG Operon (Ebersberg, Germany). Amplification was performed using a Thermocycler of the type C1000 (Bio-Rad Laboratories GmbH, Munich, Germany). Cycling conditions were 95°C for 2 min, and then 40 cycles at 95°C for 15 s and 60°C for 1 min. The PCR products were ran for 40 minutes in a 1% w/v agarose gel. A DNA ladder was also included (GeneRuler™ DNA Ladder Mix, Thermo Fisher Scientific, Waltham, USA).